Stratification stability of tropical lakes and their responses to climatic changes: Lake Towuti (Indonesia)

A THESIS

SUBMITTED TO THE FACULTY OF THE GRADUATE SCHOOL

OF THE UNIVERSITY OF MINNESOTA

BY

Tongyao Pu

IN PARTIAL FULFILLMENT OF THE REQUIREMENTS

FOR THE DEGREE OF

MASTER OF SCIENCE

Sergei Katsev

Jan, 2023

Acknowledgements

There are many people that have earned my gratitude for their contribution to my time in graduate school.

Dr. Sergei Katsev, being my academic advisor, has provided me with an enormous amount of help during my master's. He guided me to see the big research picture; asked me important questions; answered my questions patiently; and helped review and revise my thesis multiple times. Sergei is also very supportive for my career development. He advised me in attending conferences and helped me advertise myself to recruiters.

My committee members, Dr. Sam Kelly, Dr. Chan Lan Chun, and Dr. Byron Steinman came up with very interesting questions. Their suggestions are inspiring but practical, which greatly improved the current thesis content compared to the previous version.

Dr. James Russell, Dr. Doug Haffner, and Dr. Sean Crowe have provided me with long term, high quality data they have collected from Lake Towuti. Without their help, the simulations of Lake Towuti will be more foggy.

My master's experience cannot be separated from the amazing courses I had. Physical Limnology taught by Dr. Jay Austin, Fluid Dynamics taught by Dr. Sam Kelly, Data Analysis taught by Dr. Rik Gran, and Environmental Modeling taught by Dr. Nate Johnson all helped me build up my knowledge and skills to support my research work.

I also met countless wonderful people who made Duluth feel like a second home to me, especially my friends from the WRS and the physics department, and my lovely students. I am also grateful to have the chance to cat-sit Chandler, Sherbert, and Neko. These wonderful companions greatly reduced my sense of loneliness during long and dreadful holiday seasons. Unfortunately, Sherbert passed away shortly after my defense. This brought me great sadness. I will forever remember him.

Last but not least, my parents, Jianying Xia and Zhifeng Pu, are very supportive of my education, both financially and mentally. My grandma, Jinhua Li, who raised me growing up, is also very very supportive of my decisions. Unfortunately, we have not been able to get together for 3.5 years due to COVID. I hope we will see each other again soon!

Abstract

Tropical lakes have different physical dynamics than temperate lakes. They are less likely to experience thermal convection and can be permanently stratified by temperature gradients alone (thermogenic meromixis). Climate research suggests that tropical lakes are most susceptible to increasing surface temperature and stratification with future prediction of increasing air temperature. Tropical meromictic lakes are also important sites for paleoclimate research, as the anoxic and stagnant bottom layer preserves laminated sediments. Ancient Lake Towuti, located in Sulawesi island in Indonesia, is believed to be meromictic sustained without profound salinity gradient. This project aims to investigate the strength and dynamics of thermogenic meromixis in tropical lakes. To address this problem, it simulates the physical dynamics of the lake via the use of a 1-D k-ε hydrodynamic model Simstrat. The simulations reveal that Lake Towuti may be oligomictic rather than meromictic, as was previously assumed. More generally, tropical lakes much deeper than 80 m are likely to be oligo- or meromictic, whereas shallower lakes are likely to be warm monomictic. Air temperature stands out to be the most influential meteorological variable affecting stratification. Oligomixis may be regulated by a negative feedback that plays out over multiple years: A full water column mixing event will decrease the bottom water temperature of a lake and eventually increase surface-bottom temperature difference and average stability. This leads to increasing difficulties for whole-water column mixing. The temporal variation in the Lake Towuti stratification is only weakly correlated with the ENSO index. During the Last Glacial Maximum (LGM), Lake Towuti likely experienced colder and drier climate, which lowered lake level, and induced more frequent whole-water column mixing. A 1-D biogeochemical reaction-transport model, which was provided with the output of hydrodynamic simulations for the intensity of turbulent mixing, further confirmed a possibility of the whole water column mixing in Lake Towuti as recently as 2008. A weak

mixing event lasting a few weeks during the dry season would be consistent with the observed chemical profiles of O_2, H_2S, and Fe^{2+}. Coexisting dissolved iron and hydrogen sulfide at low concentrations (few $\mu mol\,L^{-1}$) likely indicate observations reflecting a transient state. Findings suggest that, under the future climate characterized by warmer air temperatures, Lake Towuti is likely to be more stable. Stronger stability and isolation of monimolimnion water would lead to further accumulation of dissolved iron. Similar tropical lakes whose stability are controlled primarily by water temperature are expected to have increasing stability in the future as well.

Contents

List of Tables

List of Figures

Chapter 1

Introduction

1.1 Physical Stratification of Lakes

Physical stratification is one of the important characteristics of a lake. The density of water is affected by temperature and the concentrations of solutes, the distributions of which within the lake are influenced by mixing rates. A strong density gradient within the water column results in stratification, creating horizontal layers with different physical and chemical properties.

Density gradients restrict vertical transport of chemicals and organisms in the water column, modify chemical conditions, affect reaction rates, and influence the way minerals and biomarkers become preserved in the sediment. Changes in stratification patterns strongly affect the functioning of lake ecosystems by controlling the transport rates of nutrients and oxygen, and the distributions of plankton (Woolway et al., 2021). Change of stratification can even lead to catastrophic events. For example, shoaling of deep water deficient in dissolved oxygen can lead to fish kills (Fukushima et al., 2017). In rare cases, release of accumulated carbon dioxide as a result of destabilization of stratification can asphyxiate humans and livestock, such as in the 1984 Lake Monoun (Sigurdsson et al., 1987) and 1986 Lake Nyos (Kling et al., 1989)

disaster.

Most water bodies stratify vertically for some periods of time, followed by periods of mixing. Based on the frequency of mixing and the type of stratification, lakes are classified into amictic, cold monomictic, dimictic, warm monomictic, oligomictic, and polymictic (Hutchinson and Löffler, 1956). Amictic lakes are later believed to be a category of meromictic lakes (Walker and Likens, 1975). Permanent stratification (meromixis) in lakes is a special case of stratification ('mero-' stands for 'partial'). In meromictic lakes, the upper part (mixolimnion) of a lake mixes and stratifies based on the local climate conditions, while the bottom part (monimolimnion) stays undisturbed. Prolonged stability limits the fluxes of energy and matter into the monimolimnion (Boehrer et al., 2017). As a result, chemical composition becomes very different between the surface and the bottom parts of the lake.

Walker and Likens (1975) classified the mechanisms by which meromixis is created into ectogenesis and endogenesis. Ectogenesis is established by an external inflow of freshwater at the surface or an inflow of denser water at depth. Endogenesis is generated by a lake's internal processes of accumulating salinity. In most meromictic lakes, whether ectogenic or endogenic, stratification is sustained by a salinity gradient that prevents water mixing between the mixolimnion and monimolimnion. However, some tropical lakes can be meromictic without a strong salinity gradient. Katsev et al. (2010) termed the phenomenon 'thermogenic meromixis'. Deep tropical lakes are known to be stabilized by a thermal gradient alone. Examples include Lake Matano. Unlike their temperate counterparts, they do not experience thermal convection that becomes more likely as the surface water approaches the temperature of maximum density of 4 °C (Katsev et al., 2017).

Table 1.1 lists tropical meromictic lakes, with their surface area A_0, maximum depth z_m, and relative depth z_r ($z_r = \frac{50 * z_m * \sqrt{\pi}}{\sqrt{A_0}}$, Walker and Likens (1975)). The relative depth metric was developed for mid-latitude lakes as a simple predictor for a lake's mixing status. Lakes with

$z_r > 4\%$ were suggested to be likely seasonally or permanently stratified. This categorization, however, does not work for tropical lakes. Only three out of nine tropical meromictic lakes mentioned in Table 1.1 have z_r greater than 4 $\%$. This table also lists some mechanisms for establishing permanent stratification, based on available information. It could be seen that tropical meromictic lakes are dynamic with drastically different shape, size, and properties.

Many large deep tropical lakes are located in tectonic depressions that existed for hundreds of thousands of years. Such lakes accumulate thick piles of sediments that contain valuable records of past climates. Meromixis and anoxia in such lakes preserve laminated sediments (Anderson, 1985), which preserve detailed chronology. Thus, such lakes often become sites of paleoclimate research. For example, the International Continental Scientific Drilling Program (ICDP, https://www.icdp-online.org/projects/) has funded projects on the East African lakes Malawi and Tanganyika, and the Indonesian lake, Towuti.

The stratification status of a lake is often linked to its climate, which determines the heat and momentum fluxes received by the lake's surface. The surface heat fluxes are commonly subdivided to shortwave radiation, longwave radiation, sensible heat transfer (thermal conduction), and latent heat transfer (evaporation). These heat flux components are linked to climate variables, such as air temperature, wind speed, solar radiation, vapor pressure, and cloud cover (Imboden and Wüest, 1995). Increases in air temperature, vapor pressure, and solar radiation would lead to heat fluxes into the lake, resulting in warmer lake surface and potentially stronger stratification. Increases in wind speed lead to heat loss via negative sensible and latent heat fluxes. The wind also exerts mechanical stress at the surface of the lake, transferring momentum, which increases turbulent kinetic energy and leads to mixing (Imboden and Wüest, 1995). Thus, increasing wind speed may destabilize stratification. Cloud cover has multiple effects that partially cancel each other. Although clouds block sunlight and inhibit shortwave radiation, they also reflect more of the longwave radiation back to the Earth

Table 1.1: Selected large tropical lakes (between 23°26' S and 23°26' N) and their stratification status. Continental location is provided : AF - Africa, AS - Asia, SA - South America. Not all the currently known meromictic lakes are included in this table. Some small meromictic lakes can be found in Alcocer (2017) (Mexican lakes) and De Crop and Verschuren (2021) (Uganda lakes)

	Lake Name	Location	A_0 [km^2]	z_m [m]	z_r [%]	meromixis mechanism	reference
1	Lake Nyos	AF	1.58	208	14.66	dissolved gas	Kling et al. (1989)
2	Lake Monoun	AF	0.31	99	15.76	dissolved gas	Sigurdsson et al. (1987)
3	Lake Kivu	AF	2700	480	0.82	dissolved gas	Sommer et al. (2019)
4	Lake Sonachi	AF	0.18	7	1.46	salinity gradient	MacIntyre and Melack (1982)
5	Lake Tanganyika	AF	32900	1470	0.72	thermogenic	Chitamwebwa (1999)
6	Lake Malawi	AF	29600	706	0.36	temp and sal gradient	Wuest et al. (1996)
7	Lake Matano	AS	164	590	4.08	thermogenic	Katsev et al. (2010)
8	Lake Toba	AS	1130	505	0.013	thermogenic	Fukushima et al. (2022)
9	Lake Atitlan	SA	137	341	2.58		Rejmánková et al. (2011)
10	Lake Lanao	AS	357	122	0.0006	warm monomictic	Frey (1969)

surface.

The stratification status of a lake can change over time. The change can happen episodically or regularly. An increasing amount of research has recently focused on the effects of climate change on lake stratification. Overall, studies suggest warming air temperatures and reduction in wind speed increase lake stability in lakes around the world (Verburg and Hecky (2009), Lake Tanganyika, Africa, meromictic; Weinberger and Vetter (2012), Ammersee, Germany, dimictic; Sahoo et al. (2016), Lake Tahoe, US, warm-monomictic; Woolway et al. (2017), Võrtsjärv, Estonia, polymictic; Oleksy and Richardson (2021), Mohonk Lake, US, dimictic; Stetler et al. (2021), Crater Lake, US, meromictic; Fukushima et al. (2017), Indonesian deep tropical lakes; Woolway and Merchant (2019), lakes globally, including tropical lakes). The general patterns are that lake temperature will be increasing in the future, leading to strengthening of stratification; Stratification will be shifting from dimictic to monomictic to meromictic (Woolway and Merchant, 2019).

Although climate warming generally increases lake stratification, individual lakes may respond differently. Hambright et al. (1994) (Lake Kinneret) and Kraemer et al. (2015) (lakes around the world) summarized the importance of lake morphology and water temperature in defining the lake's response to climate change. Deeper lakes become more strongly stratified, with deeper thermoclines. The lake surface area serves a less important role. Warmer lakes will experience greater change in enhancing stratification and decreasing depth of thermocline. Richardson et al. (2017) also added the effect of water clarity in lakes. More transparent lakes tend to have greater increases in surface water temperature and stability in response to warming air temperature. Kraemer et al. (2015) points out that tropical lakes tend to be more influenced by climate change and experience stronger stratification compared to mid-latitude lakes.

1.2 Chemical Stratification

Prolonged physical stratification limits the exchange of substances between surface and bottom water. The transport of oxygen, in particular, becomes restricted. Over time, oxygen in the deep waters becomes depleted by the respiration reactions that oxidize organic matter in the water column below the density gradient.

Once oxygen is depleted, other chemical species act as electron acceptors in a sequence of redox reactions that fuel anaerobic microbial metabolisms. The sequence of organic matter mineralization reactions includes aerobic respiration, nitrate reduction, manganese reduction, iron reduction, sulfate reduction, and methanogenesis. While the sequence is generally dictated by the thermodynamic energy gain of the reactions (Froelich et al., 1979, Berner, 1981), depending on the reaction kinetics and activities of chemicals and the order of the reactions, the sequence may change. In particular, the overlap between iron reduction and sulfate reduction is commonly observed (Canfield and Thamdrup, 2009).

In anoxic environments, accumulation of dissolved ferrous iron (Fe^{2+}, a product of iron reduction) and dissolved hydrogen sulfide (H_2S, a product of sulfate reduction) are of great importance to lake geochemistry. The prevalence of either of these two species define ferruginous (Fe^{2+}-rich) or euxinic (H_2S-rich) conditions. Aqueous Fe^{2+} and H_2S co-precipitate as poorly crystalline ferrous sulfide (FeS), which matures into more stable pyrite (FeS_2). Thus, only one of the aqueous species can be present at substantial (micromolar) concentrations, as the less abundant species would precipitate out of the solution. The classification of geochemical conditions as ferruginous or euxinic varies under different research contexts. To interpret the past water column environment based on sediment record, geologists would look at the ratio of pyrite (FeS_2) to highly reactive iron (FeHR). Ratios above about 0.7 are taken as evidence of euxinic conditions, whereas those below this threshold indicate ferruginous conditions (Poulton and Canfield, 2011).

In this study, ferruginous conditions are defined as the concentration of Fe^{2+} being significantly higher than the concentration of H_2S.

Understanding what controls the relative abundances of ferrous iron and hydrogen sulfide is important in both ecological and geological contexts. In modern settings, sulfide can limit the amounts of trace metals being available for organisms. A large quantity of sulfide will generate odor and be toxic to micro and macro organisms (Shakeri Yekta et al., 2014). In past geological epochs, before oxygen accumulated in the atmosphere, the Earth's oceans were stratified and anoxic. Prevalence of ferruginous or euxinic conditions thus defined the chemistry in the Archean and Proterozoic oceans (Poulton et al., 2004, Guilbaud et al., 2015, Swanner et al., 2020).

1.3 Hydrodynamic Models

Hydrodynamic modeling simulates the movement of water based on mass, momentum, and energy conservation laws. By including mechanical forcing, such as wind drag, bottom current drag, seiche activities, and by including heat fluxes, one can simulate the dynamics of water mass (density) and temperature.

Hydrodynamic modeling (or similarly, reactive-transport modeling introduced later) can be performed at different levels of complexity. Box models simplify the system into two or more homogeneous blocks. One-dimensional models include continuous changes in water properties along the vertical dimension, but ignore horizontal variability. Two dimensional or three dimensional models allow more realistic simulations of processes, including seiche activity, wave propagation, horizontal transport of water, coastal processes etc. Adding more dimensions escalates the complexity of models and can exhaust computational power quickly. 1-D models are often used for studies of vertical mixing in lakes where horizontal variability is limited, such as in small and medium-sized lakes.

Multiple 1-D hydrodynamic lake models have been developed. Some of the popular ones include Hostetler (Hostetler, 1987), Simstrat (Goudsmit et al., 2002), LAKEoneD (Joehnk and Umlauf, 2001), LAKE (Stepanenko and Lykossov, 2005), FLake (Mironov, 2008), MINLAKE (Fang and Stefan, 1996), and CLM4-LISSS (Subin et al., 2012). Lake Model Intercomparison Project (LakeMIP) (https://www.unige.ch/climate/lakemip/) compares these models in terms of their simulation mechanisms, accuracy, and computational efficiency (Perroud et al., 2009, Stepanenko et al., 2010, Thiery et al., 2014). The core difference in their simulation mechanisms lies in how the turbulence is estimated. The model being used in this project, Simstrat, applies the $k-\varepsilon$ turbulent closure scheme. The details of this scheme are explained in subsection 2.1.2. Simstrat also parameterizes seiche activities in one dimension, potentially improving simulation accuracy (Perroud et al., 2009).

Most of these modeling tools have been used for simulating mid-latitude lakes, such as in Switzerland and the US. Studies of tropical lakes have been rare. Exceptions are African Great Lakes: Lake Kivu (Kranenburg et al., 2020, Thiery et al., 2014, Bärenbold et al., 2022) and Lake Malawi (Likongwe et al., 2015). The difficulty in simulating tropical lakes often lies in the scarcity of direct meteorological measurements and lack of long-term continuous in-lake monitoring data for calibration and validation.

A typical hydrodynamic model application involves tethering the simulations to observational time series, and often iteratively correcting the model parameters to obtain a better fit to the highly available data. In the absence of such data, however, using a model in an exploratory fashion should be a useful way of obtaining at least qualitative understanding about the possible behaviors of the system. Performing a sensitivity analysis by observing the change in simulated solutions in response to parameter variations can be further used to understand the sensitivity of the real system to changes in the lake environment.

1.4 Reaction-Transport Biogeochemical Modeling

By simulating the effects of known biogeochemical reactions, modeling provides an inexpensive way to understand chemical dynamics in water bodies. To ensure the chemistry is realistic, the model needs to account properly for the physical transport of chemicals (Engesgaard and Christensen, 1988, Ajayi and Gupta, 2019). Reaction-transport chemistry models include such physical dynamics. For meromictic lakes, the main mechanism for chemical transport is turbulent diffusion, commonly characterized by a vertical eddy diffusivity parameter (K_z). However, measuring K_z (Jassby and Powell, 1975) is difficult in meromictic lakes, as it requires data such as continuous measurement of a tracer, or continuous and fine resolution of temperature profiles within the stagnant layer (Katsev et al., 2010).

Hydrodynamic models make up for the deficiency. The $k-\varepsilon$ turbulent closure scheme provides the simulated dynamics of K_z, which can then be applied to the chemistry model. In return, the outputs from the chemistry model, when compared to measured observational values, can inform the validity of the diffusivity values simulated by the hydrodynamic model.

1.5 Tropical Ferruginous Lake Towuti

This project uses Lake Towuti as an example, to investigate the influence of climate conditions on lake hydrodynamics, and their subsequent effects on redox chemistry dynamics.

Lake Towuti (2.75 °S, 121.5 °E) is the largest lake by surface area in the Malili Lake system on the Sulawesi island of Indonesia (Vaillant et al., 2011). It is more than 1.2 Ma old (Damanik et al., 2022). With an area of 560 km^2 and a maximum depth of 200 m (Fig 1.1), it lies in ophiolitic rocks and is surrounded by lateritic soils (Vuillemin et al., 2016, Hasberg et al., 2019).

The climate over Lake Towuti has an annual cycle of distinguishable dry and wet seasons. For Sulawesi Island, The dry season typically lasts from May to October and the wet season lasts

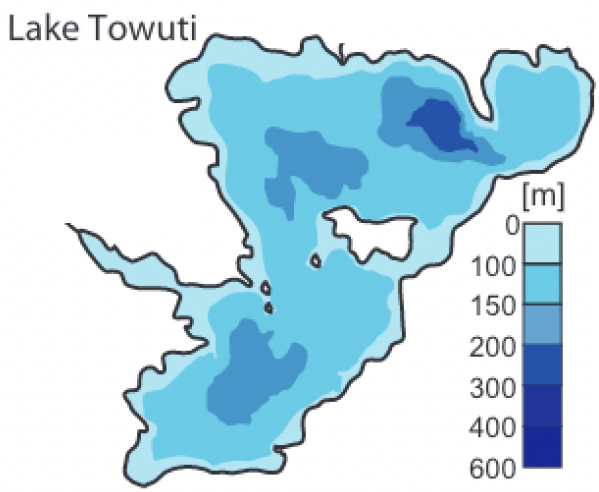

Figure 1.1: The bathymetry of Lake Towuti (modified from Russell et al. (2016)).

from November to next April. The dry season, as its name suggests, has lower precipitation, lower humidity, and lower cloud cover. It also typically comes with higher wind speed and lower air temperature. The wet season is hotter and more humid. The air temperature varies between 20 to 30 °C, with a mean of around 25 °C (Fig. 2.2). Lake Towuti is oligotrophic due to nutrient limitation, although the photosynthetically active radiation is more abundant than mid-latitude lakes. Alin and Johnson (2007) predicts that lakes in tropical regions have primary productivity of around 1000 $gC/m^2/y$. However, the primary productivity on Lake Towuti is only around 100 $gC/m^2/y$ (Dr. Sean Crowe, pers. comm.).

Lake Towuti catchment area is around 4500 km^2 (roughly measured with google map, Fig. 1.2). It is not much larger compared to the lake's surface area (561 km^2). Thus, the effect of catchment runoff is less significant in affecting the hydrodynamic process in Lake Towuti. The variation of Towuti lake level is also small. Annual fluctuation is within one meter (Fig. 1.3).

Lake Towuti is stratified primarily by a temperature gradient of a few degrees Celsius (varying seasonally between 0.5 and 3.5 °C between surface and bottom, with only a weak salinity

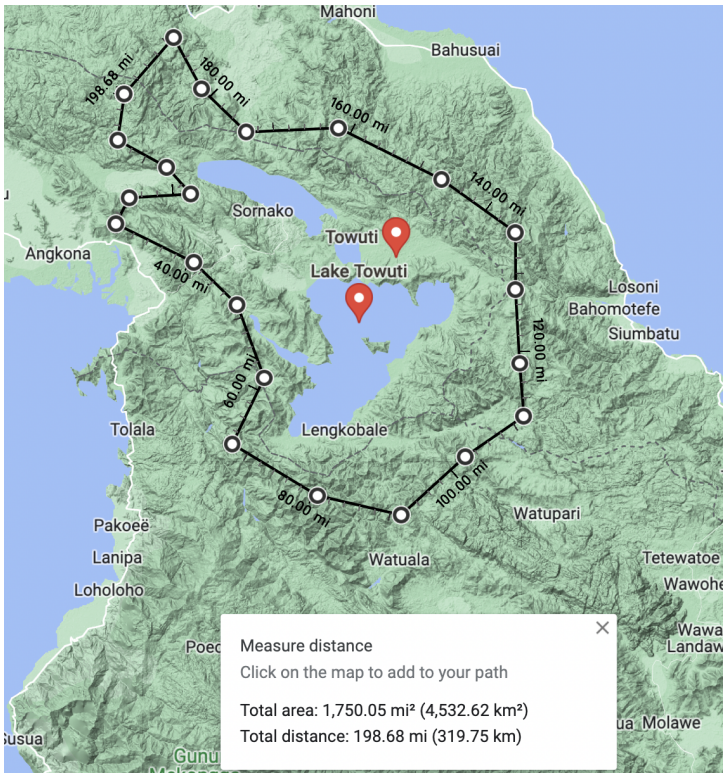

Figure 1.2: Lake Towuti catchment (including the upstream Lake Matano).

gradient. However, since there is only weak seasonality in the equatorial region, the temperature stratification may allow the lake to remain meromictic for decades, if not centuries or millennia, as is the case for the neighboring 600 m deep Lake Matano (Katsev et al., 2010). Lake Towuti has a deep thermocline that lies at around 70 m. The physical separation of the bottom waters leads to a strong chemical stratification. Oxygen is depleted below 120 m, and dissolved iron accumulates below 180 m (Costa et al., 2015).

On a longer time scale, the Lake Towuti Drilling project provides useful information in reconstructing its paleoenvironment (Russell et al., 2016). Paleoclimate proxies suggest that Lake Towuti experienced a substantially lower water level between c.a. 29 and 16 kya (Vogel et al., 2015, Goudge et al., 2017). This reduced hydrological connectivity with other Malili

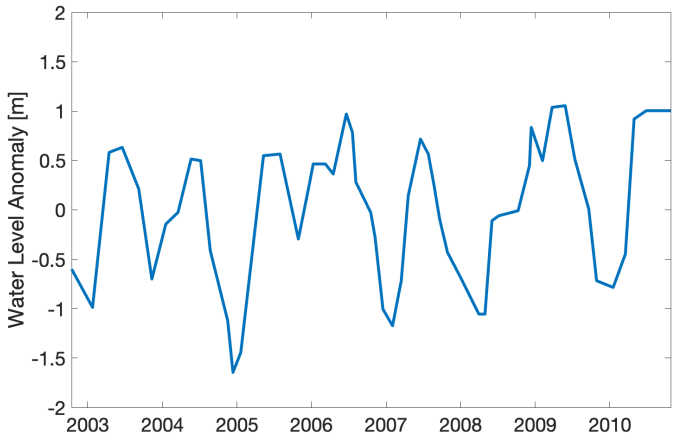

Figure 1.3: Towuti lake level via satellite altimetry Sulistioadi et al. (2015)

lakes (Costa et al., 2015). These events correspond to the global Last Glacial Maximum (LGM) period. Paleolimnological evidence, such as abundant red siderite clay (Russell et al., 2020) and Mo isotope variations (Damanik et al., 2022) suggests that the lake was mixing regularly during that period and had abundant oxygen throughout the water column. The variations in the lake's past primary production might also be made possible with changing in stratification status. Ageli et al. (2022) suggests that Lake Towuti was once dominated by productive planktonic communities. However, under modern conditions, the primary production is now dominated by benthic organisms. This can be explained by the establishing of stratification under modern conditions. This stratification blocks nutrient supply towards surface plankton communities, thus limiting the primary production.

1.6 Research Questions

In the context of meromictic tropical lakes, some of the key questions revolve around the quantitative controls on lake stratification, and the effect of them on chemical distributions.

1. What causes a tropical lake to become permanently stratified?

2. What magnitudes of changes in climate parameters might cause a meromictic lake to mix episodically, or regularly?

3. In particular, how was the physical status of Lake Towuti different during the Last Glacial Maximum?

4. How long does it take to deplete/replenish oxygen in bottom water after prolonged stratification/mixing?

5. How does the strength and persistence of stratification or mixing affect the redox chemistry in the monimolimnion?

While it is generally acknowledged that greater depths and smaller surface-to-depth ratios lead to a greater probability of meromixis, lake-specific predictions generally have not yet been possible, including stratification or destratification of a lake in the course of its geologic history. Answers to these questions hold keys to the interpretations of paleolimnological records in these lakes and linking them to the contemporary environmental conditions.

In order to answer these questions, we used a hydrodynamic model to perform an explorative study, focusing it on the possible range of hydrodynamic behaviors in Lake Towuti. By varying the climatic conditions on model input, we analyze the likely changes in Lake Towuti stratification throughout the glacial-interglacial transition. The drastic changes may be verified against the available sediment record. We then use the simulation results to infer the principal drivers for the onset of meromixis in tropical lakes.

Importantly, obtaining a realistic hydrodynamic regime provides us with a better quantification of the vertical mixing intensities (described in one-dimensional models by the turbulent eddy diffusivity parameter, K_z). The magnitude and depth variation in this parameter determine the rates of chemical transport throughout the water column, shape the vertical profiles of chemical species, and regulate their concentrations. The obtained distribution $K_z(z)$ is then

used as an input to a one-dimensional biogeochemical reaction-transport model. The simulated chemical distributions are compared against observations. Exploration of that model then allows us to conclude on the potential transitions between oxic, ferruginous (iron-rich) and euxinic (sulfide-rich) conditions in the bottom waters of Lake Towuti, throughout its Quaternary geologic history, and, by extrapolation, on the control factors for ferruginous-euxinic transitions in other water bodies.

Chapter 2

Physical Model

This chapter uses a hydrodynamic model to investigate the stability of Lake Towuti and its sensitivity to meteorological and climate conditions.

The primary questions to be answered are:

1. What causes a tropical lake to become permanently stratified?
2. What magnitudes of changes in climate parameters might cause a stably stratified lake to mix episodically, or regularly?
3. How was the physical status of Lake Towuti different during the Last Glacial Maximum (LGM), a period of substantially different climate for which paleolimnological information is available?

2.1 Methodology

2.1.1 Modeling Framework

As observational data for Lake Towuti are scarce and discontinuous, we use modeling methods to investigate the hydrodynamics and redox chemistry. The modeling framework of this project is visualized in the flowchart Fig. 2.1. The simulation of modern Lake Towuti conditions is termed as the 'nominal model', in contrast to simulations investigating the influence of changed climate and lake level conditions. The hydrodynamic model simulates the movement of water and the dynamics of water properties, such as temperature and velocity. The hydrodynamic model generates an important parameter - vertical eddy diffusivity, K_z. It is subsequently used in the chemistry model as an approximation of how chemicals get transported throughout the water column (see Chapter 3). The result of chemistry concentrations, when being compared to currently measured chemical values, serve as a confirmation to the hydrodynamic model results. We assume that chemical concentrations do not affect the physical properties of the water, thus, there is no feedback constructed from the chemistry model to the physics model.

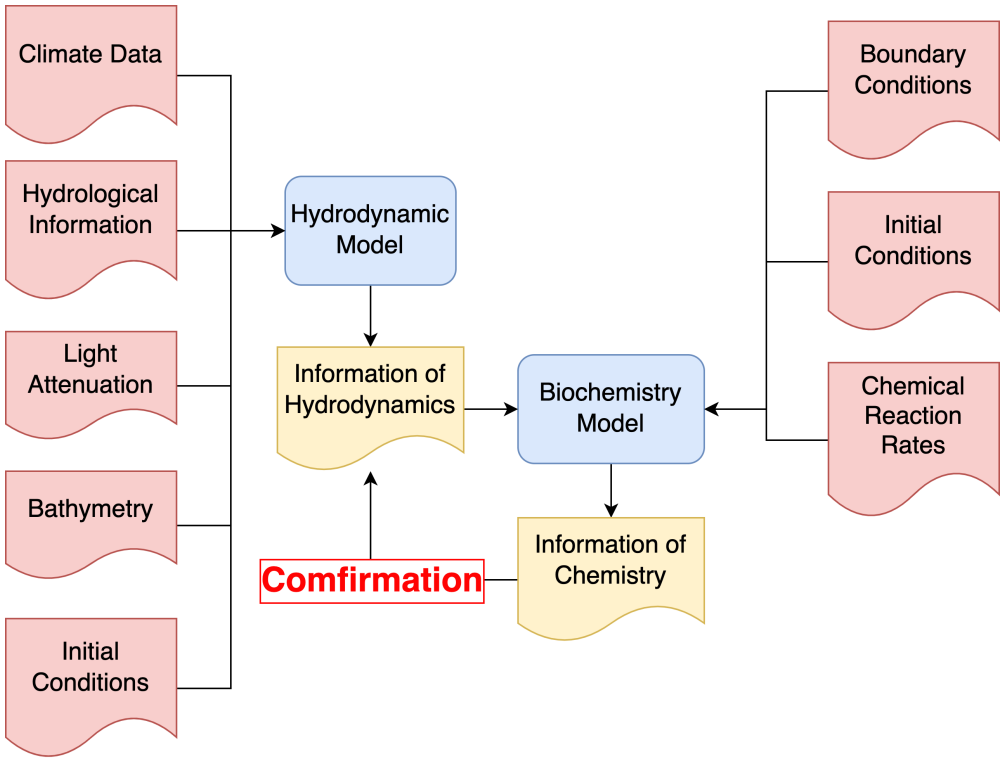

Figure 2.1: The modeling process. Rounded rectangles represent process / models; Document symbols are used to indicate inputs and outputs

2.1.2 Hydrodynamic Model

The hydrodynamics of Lake Towuti is simulated with a one-dimensional $k-\varepsilon$ model Simstrat, version 3.0 (Goudsmit et al., 2002, Gaudard et al., 2019). The model was shown (Perroud et al., 2009) to be a good choice for simulating vertical temperature profiles and thermocline positions in deep stratified lakes. It was widely used to simulate lakes in Switzerland with rigorous calibrations (Gaudard et al., 2019). It has also been applied to meromictic Lake Kivu (Thiery et al., 2014, Bärenbold et al., 2022) with success.

Main Equations

Simstrat uses the following equations to describe temperature T [°C], mean horizontal velocities u and v [$\mathrm{m\,s^{-1}}$], turbulent kinetic energy (TKE) per unit mass k [$\mathrm{J\,kg^{-1}}$] and TKE dissipation rate ε [$\mathrm{W\,kg^{-1}}$]. Depth z [m] is defined as 0 at the surface and negative downwards Goudsmit et al. (2002).

$$\frac{\partial T}{\partial t} = \frac{1}{A}\frac{\partial}{\partial z}(A(\nu_t' + \nu')\frac{\partial T}{\partial z}) + \frac{1}{\rho_0 c_p}\frac{\partial H_{sol}}{\partial z} + \frac{dA}{dz}\frac{H_{geo}}{A\rho_0 c_p} \tag{2.1}$$

$$\frac{\partial u}{\partial t} = \frac{1}{A}\frac{\partial}{\partial z}(A(\nu_t + \nu)\frac{\partial u}{\partial z}) + fv \tag{2.2}$$

$$\frac{\partial v}{\partial t} = \frac{1}{A}\frac{\partial}{\partial z}(A(\nu_t + \nu)\frac{\partial v}{\partial z}) - fu \tag{2.3}$$

$$\frac{\partial k}{\partial t} = \frac{1}{A}\frac{\partial}{\partial z}(A\nu_k\frac{\partial k}{\partial z}) + P + P_{seiche} + B - \varepsilon \tag{2.4}$$

$$\frac{\partial \varepsilon}{\partial t} = \frac{1}{A}\frac{\partial}{\partial z}(A\nu_\varepsilon\frac{\partial \varepsilon}{\partial z}) + \frac{\varepsilon}{k}(c_{\varepsilon 1}(P + P_{seiche} + c_{\varepsilon 3}B - c_{\varepsilon 2}\varepsilon)) \tag{2.5}$$

Here, ρ_0 [$\mathrm{kg\,m^{-3}}$] and c_p [$\mathrm{J\,kg^{-1}\,K^{-1}}$] are reference density and specific heat of water. A [$\mathrm{m^2}$] is the surface area of lake at depth z [m], H_{sol} [$\mathrm{W\,m^{-2}}$] is the shortwave solar radiation flux into the lake, H_{geo} [$\mathrm{W\,m^{-2}}$] is the geothermal heat flux, and f [$\mathrm{s^{-1}}$] is the Coriolis parameter. ν and ν_t are molecular and turbulent viscosity for momentum, ν' and ν_t' are molecular and turbulent diffusivity of temperature, and ν_ε and ν_k are the turbulent diffusivity of energy dissipation and TKE. These viscosity / diffusivity terms all have units of [$\mathrm{m^2\,s^{-1}}$]. P and B [$\mathrm{W\,kg^{-1}}$] represent

the kinetic energy generated from shear stress production and buoyancy production:

$$P = \nu_t((\frac{\partial u}{\partial z})^2 + (\frac{\partial v}{\partial z})^2) \tag{2.6}$$

$$B = -\nu_t' N^2 \tag{2.7}$$

where N [s^{-1}] is the buoyancy frequency defined as:

$$N = -\frac{g}{\rho_o}\frac{\partial p}{\partial z}. \tag{2.8}$$

The model also simulates the effect of seiches on turbulent kinetic energy by adding a production term P_{seiche} in equation 2.4 and 2.5. This term is an empirical fit of seiche energy as a portion from the surface and bottom stress, discussed in detail by Goudsmit et al. (2002).

The molecular viscosity for momentum is:

$$\nu = 1.5 \times 10^{-6}\ \mathrm{m^2\,s^{-1}} \tag{2.9}$$

The molecular diffusivity for temperature is:

$$\nu' = 1.5 \times 10^{-7}\ \mathrm{m^2\,s^{-1}} \tag{2.10}$$

Finally, the turbulent viscosity and diffusivity for momentum, temperature, k, and ε can be calculated with Kolmogorov-Prandtl relation. They are all linearly related to $\frac{k^2}{\varepsilon}$. Turbulent viscosity for momentum is:

$$\nu_t = c_\mu \frac{k^2}{\varepsilon} \tag{2.11}$$

Turbulent diffusivity for temperature is:

$$\nu_t' = c_\mu' \frac{k^2}{\varepsilon} \tag{2.12}$$

Turbulent diffusivity for k is:

$$\nu_k = \frac{c_\mu}{\sigma_k} \frac{k^2}{\varepsilon} \tag{2.13}$$

Turbulent diffusivity for ε is:

$$\nu_k = \frac{c_\mu}{\sigma_\varepsilon} \frac{k^2}{\varepsilon} \tag{2.14}$$

The values of the constants, c_μ, c_μ', σ_k, and σ_ε are given in Table B.1, along with other model parameters.

In summary, this model provides a 1-D approximation of mixing based on viscosity and diffusivity of momentum and temperature, which is scaled based on turbulent kinetic energy and its dissipation rate. Convection of water and the associated convective mixing is represented with greater diffusivity terms.

Simulation Configuration and Input

Inputs to the hydrodynamic model include lake bathymetry, initial distributions of temperature and salinity, light attenuation, hydrological inputs, and meteorological variables.

Lake bathymetry is defined by a hypsographic curve, the areal extent as a function of depth, at 5 meter intervals, interpolated from Fig. 1.1. The depression in the southern basin below 150 meter was excluded from the areal extent calculation because it is effectively isolated from the main deep basin. Several model runs suggest that the simulated stratification was not significantly affected by the details of lake morphology or by excluding the separate deep basin.

Initial conditions required by Simstrat includes water column temperature t [°C], salinity S [‰], horizontal velocity defined by u and v components [$\mathrm{m\,s^{-1}}$], TKE per unit mass k [$\mathrm{J\,kg^{-1}}$], and TKE dissipation rate ε [$\mathrm{W\,kg^{-1}}$]. Initial horizontal velocities are set to 0 [$\mathrm{m\,s^{-1}}$], initial k is set to 3×10^{-6} [$\mathrm{J\,kg^{-1}}$] and initial ε is set to 5×10^{-10} [$\mathrm{W\,kg^{-1}}$].

The initial temperature and salinity are obtained from CTD measurements in 2001. CTD profiles for multiple years were obtained from Drs. Sean Crowe and Doug Haffner (personal communication). These CTD profiles consist of temperature and conductivity measurements. The density of water was calculated via the equation of state (Chen and Millero, 1986):

$$\rho^0 = 0.9998395 + 6.7914 \times 10^{-5} t - 9.0894 \times 10^{-6} t^2 + 1.0171 \times 10^{-7} t^3 - 1.2846 * 10^{-4} t^4 + 1.1592 \times 10^{-11} t^5 - 5.0125 \times 10^{-14} t^6 + (8.181 \times 10^{-4} - 3.85 \times 10^{-6} t + 4.96 \times 10^{-8} t^2) S \tag{2.15}$$

where ρ^0 is the density of water at the surface with zero water pressure, aka potential density. t and S are temperature and salinity at each depth. Salinity is approximated from the measured conductivity using a simple scale function from Katsev et al. (2010) for the neighboring Lake Matano:

$$Salinity\ [g\ kg^{-1}] = 0.0010 \times Conductivity\ [\mu S\ cm^{-1}] \tag{2.16}$$

Here, conductivity is in [$\mathrm{\mu S\,cm^{-1}}$], and the resultant salinity is in [$\mathrm{g\,kg^{-1}}$].

For the initial conditions, the temperature and salinity were extrapolated from the closest available measured profiles.

The coefficient of light attenuation in the water column was estimated from the profile of the photosynthetically active radiation (PAR) measured in 2015 (Sean Crowe, personal

communication). This was done by linear fitting the log-transformed profile between 17 and 110 m depth. Lake Towuti's photic zone is very deep. Light attenuates to 1 % at approximately 60 m. This is a result of Lake Towuti being an oligotrophic lake, with few particles to scatter light. In the simulations, light attenuation was assumed to be constant throughout seasons. The magnitude of light attenuation strongly affects the depth of the simulated thermocline and is potentially important for the agreement between model and observations.

River inflow and outflow data are unavailable, but since Lake Towuti has very small catchment-to-lake area ratio, the hydrodynamics of the lake is not highly sensitive to river discharges. Several trials were conducted with different orders of magnitude of discharges (20, 7×10^7 $m^3\,s^{-1}$). The mixing pattern was not significantly affected. Thus, the default discharge values were fixed at 20 $m^3\,s^{-1}$ for both river inflow and outflow.

Surface forcing parameters required by Simstrat include zonal and meridional wind speeds, surface air temperature, surface solar radiation (after atmospheric absorption/reflection), vapor pressure, and cloud cover. These variables were obtained from ERA5 reanalysis dataset (Hersbach et al., 2020) with hourly resolution. Care was taken to only select the available land grids around Lake Towuti (121.4 °E, 2.75 °S) to avoid the nearby ocean climate. The time series of average ERA climate variables are presented in Fig. 2.2.

The monthly average of ERA5 reanalysis dataset is compared with observational data in Fig. 2.3. Meteorological observations were available for Kendari (166 km away) and Palu (300 km away) city. ERA5 reanalysis has a similar air temperature range. The wind speed is half or a quarter of that being observed in the two cities. Relative humidity from ERA5 is lower than observations during July - October. The surface shortwave radiation from the reanalysis data has a similar trend with the sunshine minutes observed in Kendari. The cloud cover is higher for ERA5 than observed. The total precipitation is within the range between Kendari and Palu.

The reanalysis data is the best choice for modeling Lake Towuti, as there is no direct

measurement of meteorology over the lake that can satisfy the time resolution requirement for model simulation. Although discrepancies exist between observational and reanalysis meteorology, there is little confidence in deciding which one best represents the real condition over the lake surface. Both of the observed weather stations are far away, and are located in different geographical environments (both Kendari and Palu are coastal cities at lower elevations).

Adequate results were obtained from the uncorrected reanalysis data, except the absorption of shortwave and longwave radiation are downscaled by a constant factor (App. B, see $p_{sw\ water}$ and p_{lw}). Other constants used in the model were set so that their values were deemed to best represent tropical lakes (App. B). Otherwise no additional calibration and correction were conducted due to the lack of long-term continuous monitoring data.

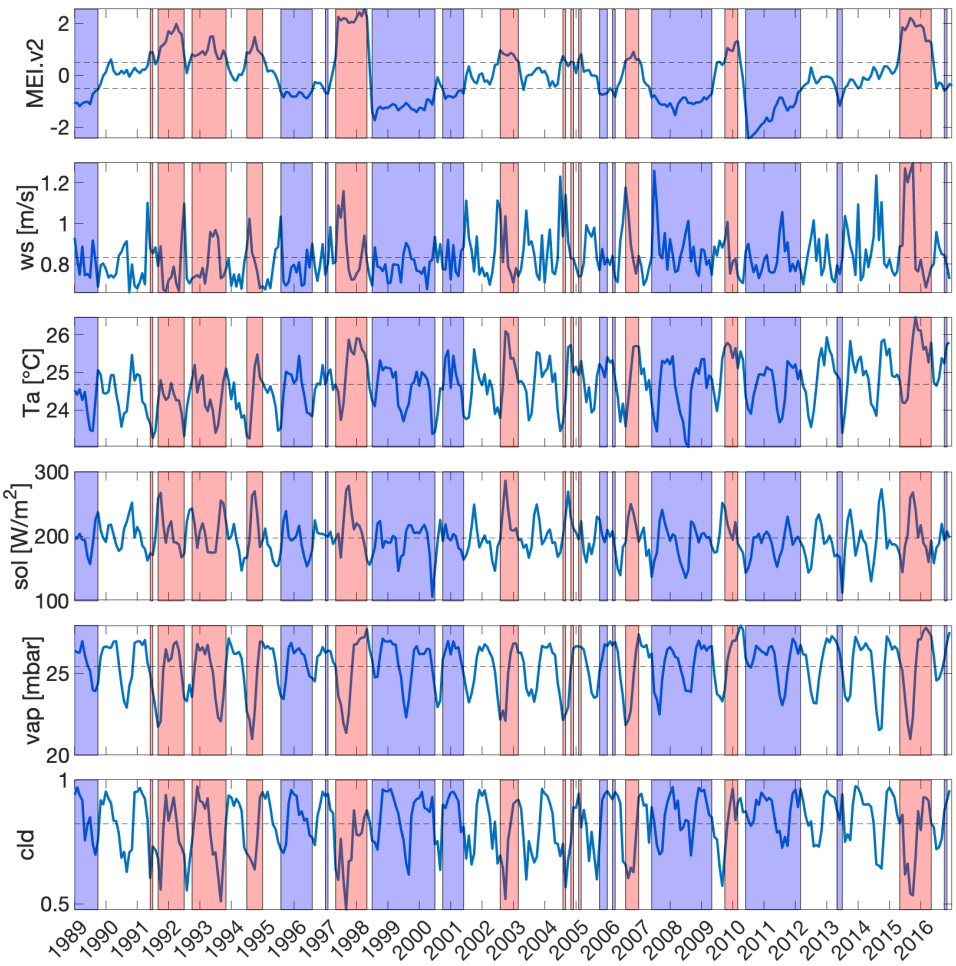

Figure 2.2: ERA5 reanalysis climate variables from 1989 to 2016, marked with ENSO events indicated by the MEI.v2 index: El Niño (MEI $>$ 0.5) are marked with red bands; La Niña (MEI $<$ -0.5) are marked with blue bands.

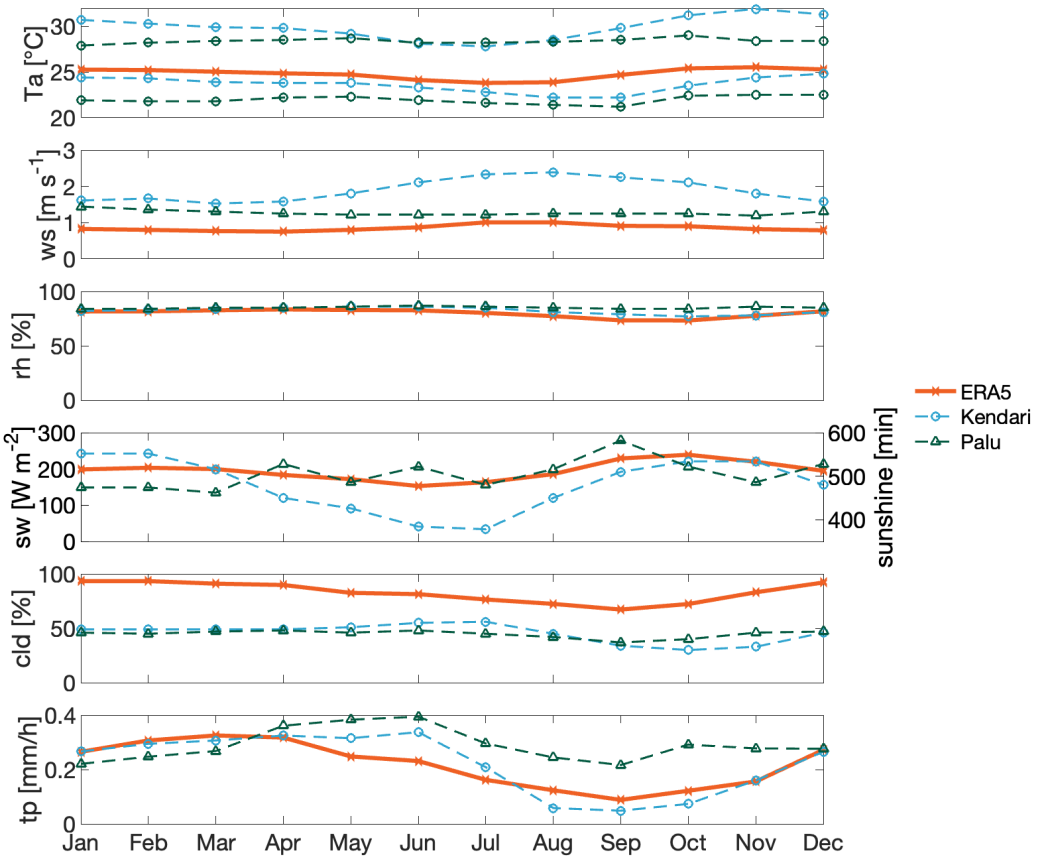

Figure 2.3: Comparison of the annual climate data around Lake Towuti from different sources. ERA5 reanalysis data are presented as mean monthly averages derived for 2000-2016. Observational data are from weather stations in Kendari and Palu city (https://www.weather-atlas.com/, year range unknown).

2.1.3 Stratification Strength Indicators

We define several indicators to quantify the strength of stratification of the entire water column of the lake. We use temperature difference indicator (TDI), heat content indicator (HCI), and Schmidt Stability index (SSI) as characteristics of the entire water column at any given time. The weakest temperature difference (WTD) and maximum buoyancy frequency (MBF) are used to characterize the weakest and the strongest instances of stratification over the entire simulated period.

The temperature difference indicator (TDI) is calculated as the difference between the maximum temperature and minimum temperature in a water column. This is typically the difference between lake surface temperature and bottom temperature. A TDI around zero indicates that the water column has uniform temperature, indicating a whole water column mixing.

$$TDI(t) = \max_{z}(T(z,t)) - \min_{z}(T(z,t)) \tag{2.17}$$

The Weakest Temperature Difference (WTD) is defined as the smallest temperature difference indicator (TDI) in the water column throughout the whole simulated time series:

$$WTD = \min_{t}(TDI) \tag{2.18}$$

A WTD of zero would indicate the existence of a homogeneous temperature distribution throughout the water column at least once during the simulation, indicative of the whole-water column mixing.

The Maximum Buoyancy Frequency (MBF) is the maximum Brunt-Väisälä frequency squared (N^2) anywhere in the water column. MBF characterizes the stability at the thermocline. Higher

MBF indicates a more stable thermocline being achieved during the simulation run:

$$MBF = \max_{t,z}(N^2(z,t)) \tag{2.19}$$

The Schmidt Stability (SS) characterizes the stability of the water column based on the density gradient. It is defined as (Idso, 1973) :

$$SS = \frac{g}{A_0} \int_{z=z_d}^{z=0} (z - z_g)\, A_z\, (\rho - \bar{\rho})\, dz \tag{2.20}$$

It represents the energy needed to mix the water column from the surface down to a depth z_d. The Schmidt Stability index (SSI) is the SS taken to the maximum depth. Here A_0 is the lake surface area, A_z is the areal extent at depth z, and z_g is the depth of the center of the mass, calculated by:

$$z_g = \frac{\int_{z=z_d}^{z=0} \rho\, A_z\, z\, dz}{\int_{z=z_d}^{z=0} \rho\, A_z\, dz} \tag{2.21}$$

and $\bar{\rho}$ is the average density of the water column, calculated by:

$$\bar{\rho} = \frac{\int_{z=z_d}^{z=0} \rho\, A_z\, dz}{\int_{z=z_d}^{z=0} A_z\, dz} \tag{2.22}$$

The Heat Content (HC) characterizes the susceptibility of the water column to mixing under changes in heat fluxes. It is defined as the water heat content in the water column above depth z_d:

$$HC = \frac{1}{A_0} \int_{z=z_d}^{z=0} \rho\, c_w\, (T - T_0)\, A_z\, dz \tag{2.23}$$

where T is the *in situ* temperature. T_0 is an arbitrarily chosen reference temperature (28 °C if not state otherwise), c_w is the specific heat of water, 4200 [$\mathrm{J\,kg^{-1}\,°C^{-1}}$]. The Heat content indicator (HCI) is the heat content of the entire water column.

To eliminate the effects of the initial spin up period for the model, the first year of the simulation was usually excluded from the indicator analyses.

2.1.4 Sensitivity Test

A Monte Carlo method was used to test the sensitivity of the model simulated stability to climate variables. Multiple climate variables were varied randomly at the same time, and the same model simulations were repeated for 100 randomized parameter sets. The parameters were drawn from normal distributions, which covered the realistic ranges of the respected variables. The standard deviations (σ), chosen to represent relevant environmental ranges, are listed in Table 2.1. For the wind speeds u and v, the normally-distributed randomization factors were used multiplicatively, rather than additively. The average values of the meteorological variables are calculated and compared with stratification indicators (WTD and MBF) calculated for each model run. As the climate variables may be coupled among themselves in reality, the distributions that characterize their real variability may deviate from the independently chosen normal distributions used here. The Monte Carlo analysis serves as an exploration for understanding the effects of climate variables on hydrodynamic circulation in tropical lakes.

Variables	distribution	standard deviation	unit
Wind speed	multiply Gaussian	0.4	$m\ s^{-1}$
Air temperature	Gaussian	1.5	°C
Vapor pressure	Gaussian	1	mbar
Cloud cover	Gaussian	0.1	%

Table 2.1: Variations in meteorological variables used in the Monte Carlo analysis.

2.1.5 Correlation with the ENSO Climate Index

Located in the tropical west Pacific, Lake Towuti might be susceptible to the variations of large climate cycles, such as El Niño-Southern Oscillation (ENSO). The correlation of the ENSO index, MEI.v2 (https://psl.noaa.gov/enso/mei/) and the model simulated SSI has been investigated by cross correlation. This is conducted by MATLAB normalized cross correlation function, with inputs of the MEI.v2 index and SSI(t) from the nominal Simstrat simulation run (2-hour resolution). The normalized cross correlation generates Pearson correlation coefficient r as a function of lag. Positive lag indicates MEI.v2 prior to SSI. Positive correlation coefficient indicates the El Niño corresponds to strong SSI or La Niña corresponds to weak SSI. A negative correlation coefficient indicates the opposite effect, that is, El Niño corresponds to weak SSI or La Niña corresponds to strong SSI.

2.1.6 Lake Towuti in the Last Glacial Maximum

Stratification of Lake Towuti during the Last Glacial Maximum was simulated to establish correspondence with existing sediment records (Russell et al., 2020). During the Last Glacial Maximum (LGM), the average air temperature was estimated to be 4 °C cooler, relative humidity 15 % lower, and wind speed 2 – 3 times higher than modern conditions (estimated by Dr. James Russell, personal communication).

Simulation	Climate	Lake Level
1	Modern	100
2	Modern	150
3	Modern	190
4	LGM	100
5	LGM	150
6	LGM	190

Table 2.2: Simulation runs for investigating the effect of LGM conditions.

2.2 Results

2.2.1 Stratification of Lake Towuti

The simulated temperature distributions reproduce the essential features of the observational data, despite the input data being approximated from reanalysis with minimal calibration. Simulated water temperatures range between 28 °C at the bottom and 30 °C at the surface, matching the observational ranges. The seasonal thermocline deepens during the wet season, from 40 to 60 m deep. The model somewhat underestimates surface water temperatures and overestimates the depth of the thermocline compared to the mooring observations from 2012-2015 (Fig. 2.5). The overall differences between the mooring data and the simulation, however, do not exceed 1 °C (Fig. 2.6).

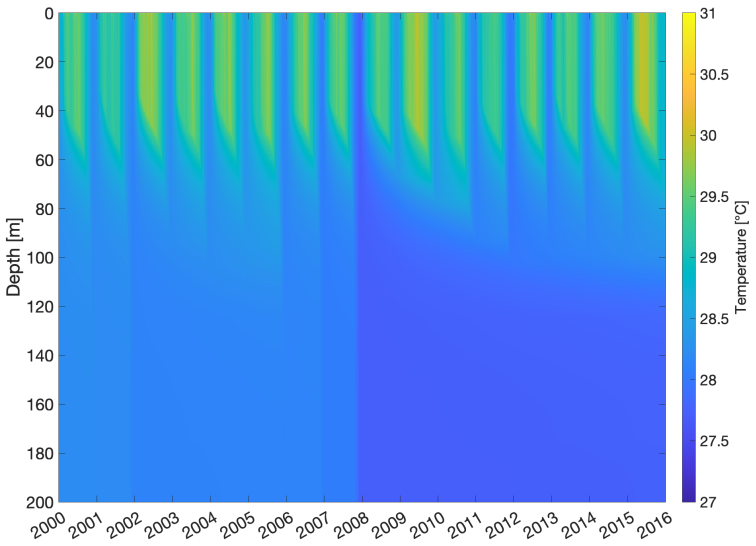

Figure 2.4: Temperature distributions and evolution in Lake Towuti simulated using the unmodified ERA5 reanalysis meteorological data as model input.

The long term simulation (Fig. 2.4) showed some temperature variability in the deep monimolimnion that was not captured by shorter term mooring observations (Fig. 2.5) but was

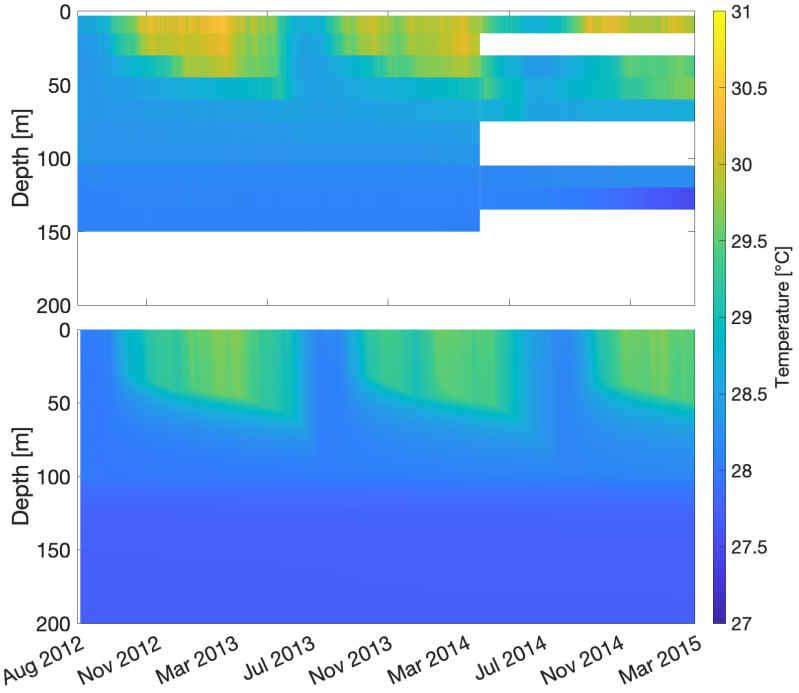

Figure 2.5: Comparison of simulations with the temperature data from a moored instrument array (Dr. James Russell, pers. comm.; observational data after June 2014 have less confidence due to instrumentation problems).

recorded in the discrete CTD profiles taken over 2000-2009 (Fig. 2.7). Lake Towuti's bottom layer was previously assumed to have been isolated from surface waters, with heat exchange occurring only slowly, via diffusion across a stable thermocline. However, model outputs suggest one or more potential mixing events. The model predicts mixing in 2001 and 2002, with temperature at the bottom of the lake cooling down as a result. From the 2002 dry season onward, stratification became established and the bottom water slowly warmed up, as heat diffused downward from the epilimnion. In the 2007/2008 dry season, the water column mixed again, lowering the bottom lake temperature by almost half a degree, from the original 28 °C to 27.5 °C. The simulated temperature profiles from these cooling and warming events seem to match the available CTD profiles from 2000 to 2009 (Fig. 2.7). As the CTD profiles represent

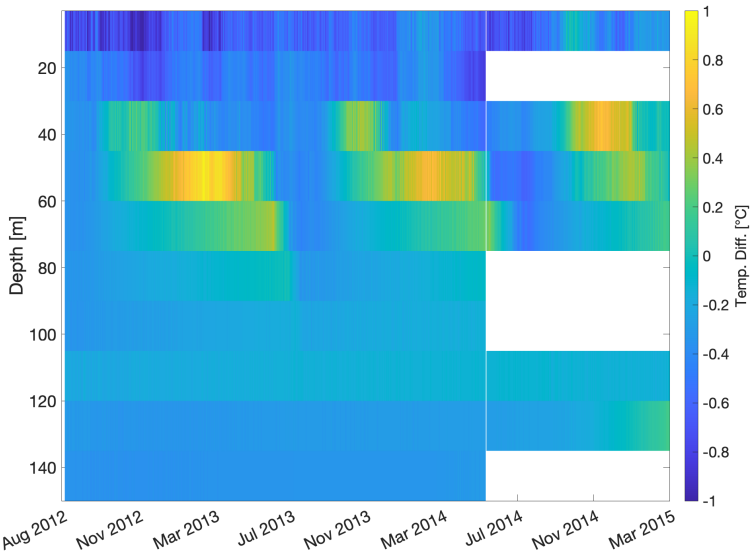

Figure 2.6: Residuals from the model (model minus mooring temperature). Warm color indicates warmer simulated temperature, colder color indicates colder simulated temperature compared to the observation

discrete moments of time and were not taken in the same seasons, inferring changes from such observations alone is difficult. The simulations illustrate the corresponding dynamics that happened over multiple seasons. In particular, they show that the cooler water temperature in the deep water observed in the 2009 CTD profile compared to the 2006 and earlier profiles is most likely the result of a deep mixing event in the dry season of 2008.

The simulation provides information on the dynamics of the heat content and the stability of the lake (Fig. 2.8). A complete mixing of the lake would homogenize the temperature in a water column, corresponding to zero TDI and zero SSI. A complete mixing should be associated with negative surface heat flux, which cools down the entire water column. Thus, the average HCI would also decrease. After the 2008 mixing event, TDI and SSI rebounded and their average values increased compared to the pre-2008 state. This indicates that the thermal gradient in the lake increased after mixing. The more stable stratification lasted until the end of the simulation

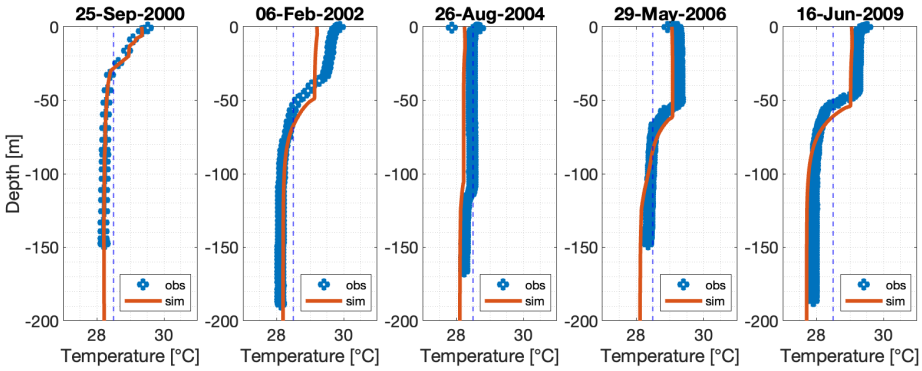

Figure 2.7: Comparison between observational CTD temperature profiles and modeled profiles at the corresponding time. Vertical dashed lines represent 28.5 °C. It is plotted to provide an easy comparison between different CTD profiles.

time frame. Cooling of the bottom water thus made the lake more difficult to be fully mixed again.

Simstrat also provides information on the lake surface heat flux. Fig. 2.9 shows the heat flux in a typical stratified year (2012). Shortwave and longwave radiation from the sky provide the positive inflow of heat. Longwave radiation out from the lake, sensible heat flux, and latent heat flux make up for the negative outflow of heat. Overall, the seasonal variations of shortwave and downward longwave radiation are the most significant components of the heat flux balance, followed by the variations in latent heat flux.

The surface heat fluxes are affected by the meteorological variables. Surface shortwave radiation, which is the incoming radiation from the sun, depends on the time of year and the reflection and absorption of light by the atmosphere. Thus, when the cloud cover or relative humidity are higher, the amount of shortwave radiation reaching the lake surface is reduced. This leads to lower shortwave radiation inputs from April to July, and higher radiation from August to November. Longwave radiation from the sky (or longwave in) is linked to air temperature and humidity. Higher air temperature and humidity are usually observed during the wet season. Thus, incoming longwave radiation is greater during the wet season, between

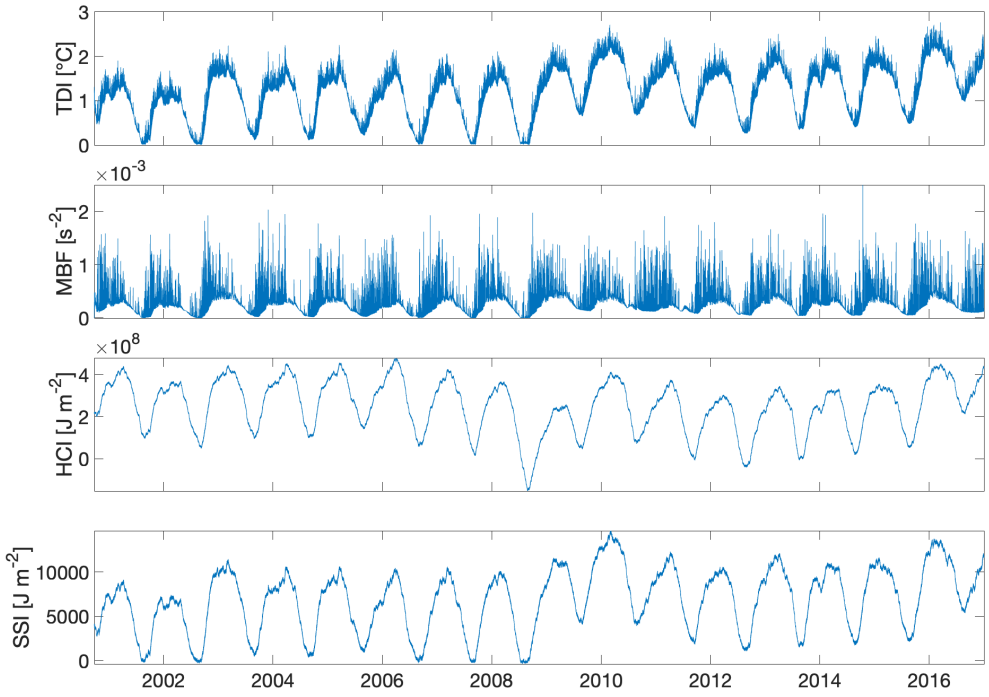

Figure 2.8: The simulated time series for the overall stratification indicators: temperature difference indicator (TDI), maximum buoyancy frequency (MBF), heat content indicator (HCI), and Schmidt Stability index (SSI).

November and June of the following year. Outbound longwave radiation emitted by the lake follows Planck's law (black-body radiation), and is only related to the surface water temperature. Since the surface water temperature is warmer from November to April, that is when the longwave radiation out from the lake is greatest (more negative). Sensible and latent heat are determined by wind speed, air temperature, water temperature, and humidity (Imboden and Wüest, 1995). As water temperature is always warmer than air temperature, these two fluxes are always negative. Greater wind speed and lower humidity usually occur during the dry season, leading to more negative sensible and latent heat fluxes. However, during the dry season, the air temperature and water temperature are both cooler, leading to an opposite effect.

On balance, air temperature and water temperature exert a more significant influence on the sensible and latent heat fluxes.

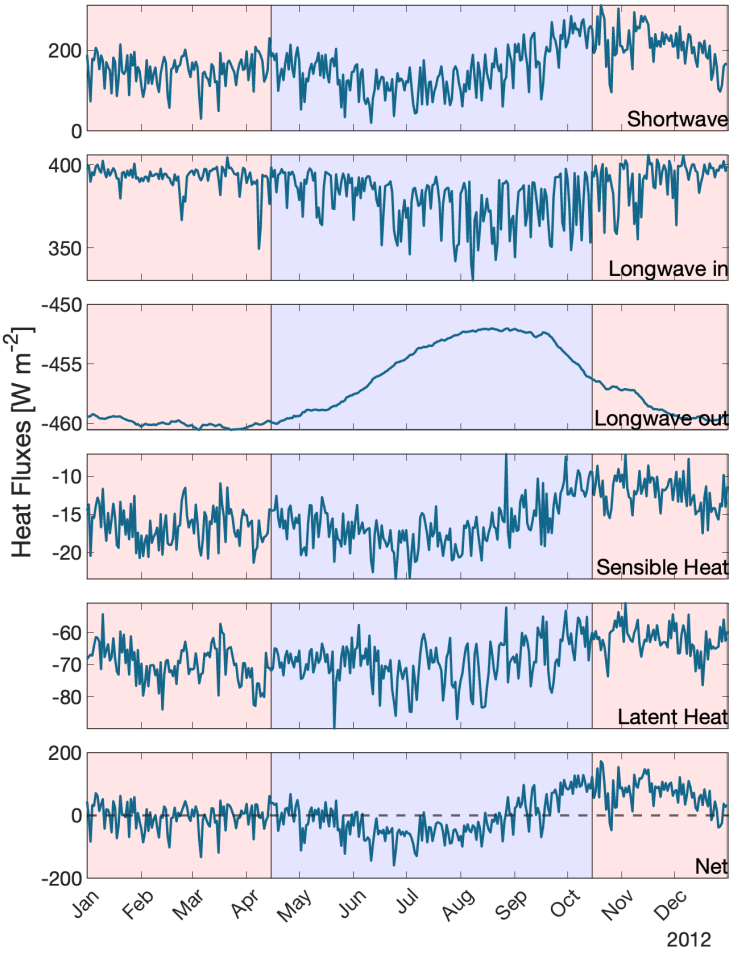

Figure 2.9: Heat fluxes across the lake surface calculated by Simstrat in 2012. From top to bottom: shortwave radiation, longwave radiation reflected from sky into the lake (longwave in), longwave radiation from lake into the atmosphere (longwave out), sensible heat, latent heat, and the net heat flux. Red shaded regions mark a typical Sulawesi wet season, and blue shades indicate a typical dry season.

Fig. 2.10 presents the correlation between the monthly averages of the climate variables from

the ERA5 reanalysis (same as the model inputs) and the monthly averages of the SSI. Each data point represents a monthly sample from the nominal simulation. The corresponding correlation coefficients and p-values are listed in Table 2.3 (note that the data points, being from the same simulation, are not statistically independent, hence these statistical measures are provided only for illustration). The Schmidt Stability index correlates with most of the climate variables. The correlation is stronger with air temperature, vapor pressure, and cloud cover, and weaker with wind speed. The correlation with solar radiation is not significant. This suggests that the incidents of weaker stratification (low SSI) are associated mostly with cooler air temperatures and drier conditions. Higher winds also occur at the times of weaker stratification. Note that the correlation here does not necessarily indicate that a particular climate variable controls the stability (causality), as they co-vary among themselves. In the Monte Carlo simulations in Fig. 2.13, where values of the climate variables were varied independently, vapor pressure and cloud cover by themselves did not significantly affect lake stability. Lower vapor pressure and lower cloud cover are, however, associated with the period's lower air temperatures (dry season) in the Lake Towuti region.

SSI correlated with	r	p
Wind Speed	-0.245*	0.00001
Air Temperature	0.696*	0.00000
Solar Radiation	-0.072	0.19087
Vapor Pressure	0.826*	0.00000
Cloud Cover	0.653*	0.00000

Table 2.3: Correlation between ERA5 climate variables and the SSI of Simstrat simulation run with them as inputs.

We also inspected the connection between the strength of the lake stratification and the regional climate variations. The response of lake stratification to large-scale variations, specifically, El Niño-Southern Oscillation (ENSO), is not straightforward. (Fig. 2.11). Several SSI troughs do follow the periods of negative MEI.v2 index, such as from year 2000 to year 2008. However,

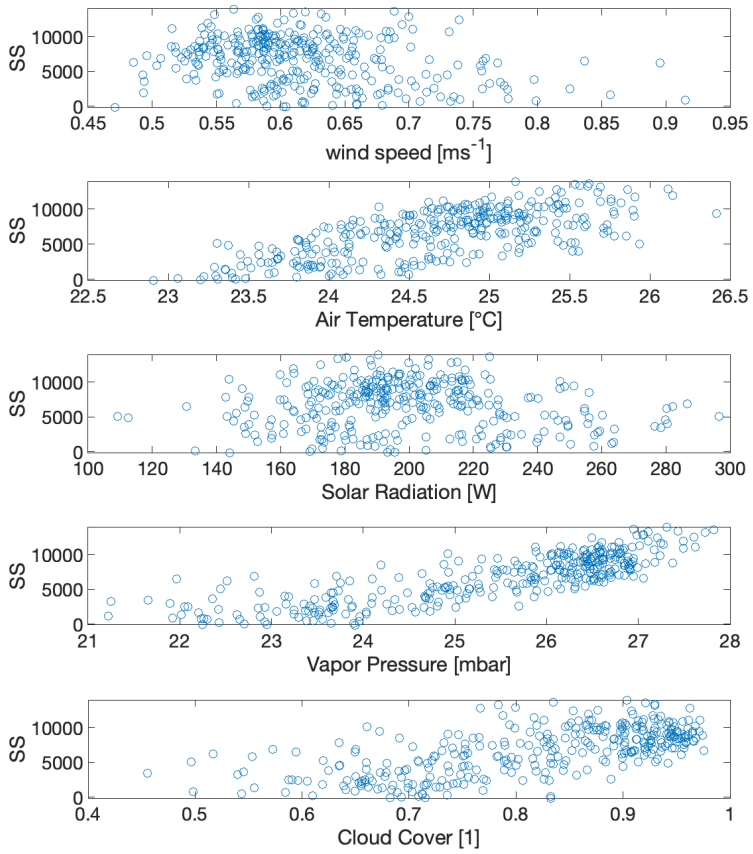

Figure 2.10: Scatter plots of SSI against model input climate variables (from ERA5 reanalysis). Because the (monthly) data points correspond to monthly averages, a brief mixing of the water column corresponds to low values of SSI but not necessarily zero.

anti-correlations between SSI and MEI.v2 index are also observed, such as from 1990 to 1995. Similarly, periods of high stability (year 1997, Year 2003, Year 2010, and year 2016) correspond with positive MEI.v2 index (i.e. El Niño periods.), though some (shorter) periods of high MEI.v2 did not apparently lead to greater stability (years 2005).

Fig. 2.12 shows the cross-correlation function between the ENSO index and the simulated

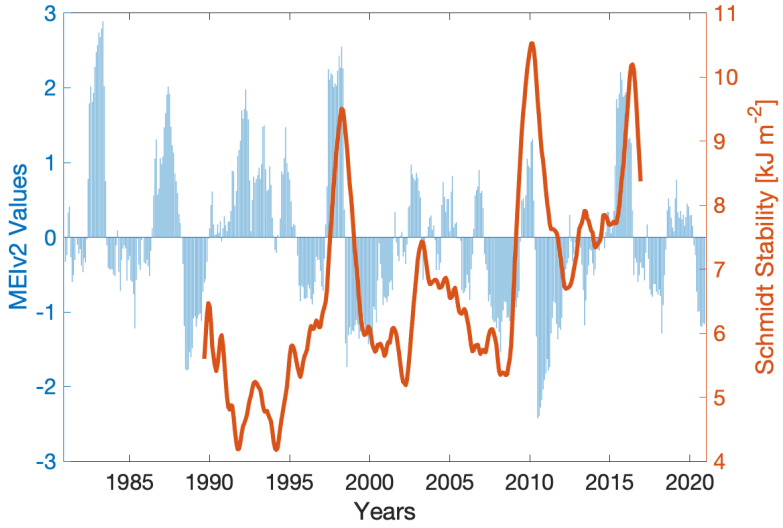

Figure 2.11: The MEI.v2 index of ENSO (> 0.5 - El Niño, < -0.5 - La Niña) and the moving (12 months) mean of the Schmidt Stability (SSI) from the simulation.

lake stability, represented by SSI. The horizontal axis is the time lag in months. Negative time lag corresponds to the ENSO indicators leading the SSI. Positive correlation coefficient would indicate the El Niño events being associated with higher lake stability and/or La Niña events being associated with lower stability. Negative correlation would indicate the opposite relationship. The cross-correlation shows that the higher (lower) values of the MEI.v2 index corresponds to increased (decreased) stability about four months later. However, the correlation is not strong, for reasons discussed later (see Discussion 2.3.5). The correlations between MEI.v2 index and the individual climate variables are included in Fig. D.4 for reference.

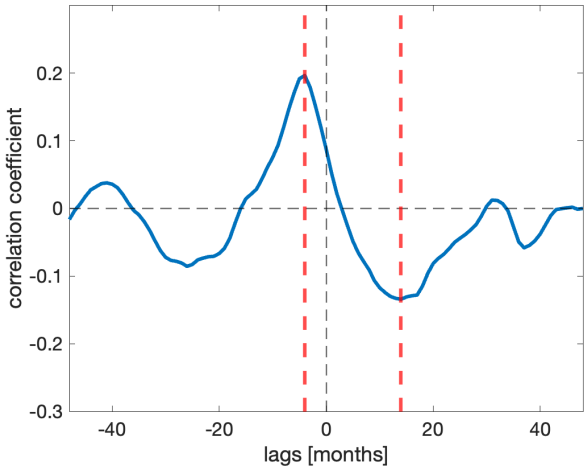

Figure 2.12: Normalized cross correlation between the MEI.v2 index and unfiltered Schmidt Stability index (SSI) (all detrended). This figure shows that the high MEI.v2 indexes, i.e. El Niño events, are correlated with weaker stability simulated in the model, and vice versa for La Niña events. The maximum positive correlation occurs with a -4 month lag with the correlation coefficient of 0.197. The maximum negative correlation occurs with a 14 months lag with the correlation coefficient of 0.134. These are not strong correlations. If ENSO climate variation is a precursor for the lake status change, the effect occurs approximately 4 months later.

2.2.2 Sensitivity Test Results

The Monte Carlo sensitivity analysis illustrates the effects of individual meteorological variables on lake stratification (Fig. 2.13, 2.14). Wind speed and air temperature have the most significant effects on Lake Towuti's stratification strength. As expected, average wind speed correlates negatively with the stratification strength while air temperature has a positive correlation. In contrast to the single-simulation results in Fig. 2.10, vapor pressure and cloud cover individually do not have strong effects on stratification, when their effects are investigated independently in Monte-Carlo runs of the model. The sensitivity test suggests the typical magnitudes of climate variables that would be required for long-term stratification or, alternatively, might lead to whole-water column mixing (as indicated by WTD). For Lake Towuti, the lake is likely to experience complete mixing if the average wind speed is above 2

$m\,s^{-1}$ (doubled from ERA5 averages), or when the average air temperature is below 23 °C (1–2 °C cooler than ERA5 averages). On the other hand, if the average air temperature exceeds 27 °C, the stratification of the lake is likely to persist for the whole simulated period. Higher air temperatures also lead to stronger thermocline during the stratified wet season (as indicated by MBF). Wind has a weak negative effect on the strength of the thermocline. In this project, wind speed is used to correlate with lake stability. However, in the future, it will be more sensible to use wind power (related to cubed wind speed) for the purpose of this comparison since wind power more linearly controls energy fluxes.

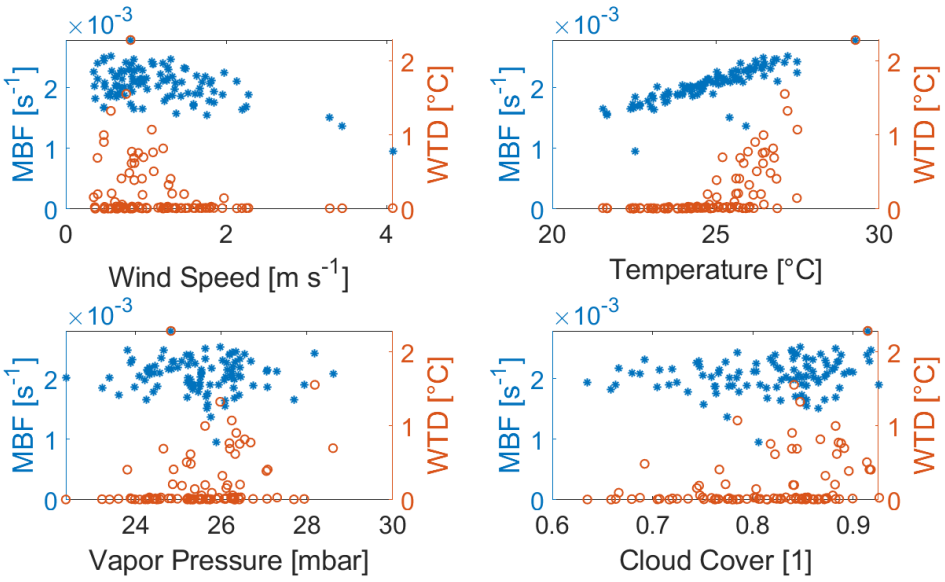

Figure 2.13: Correlation between the MBF indicator for the maximum strength of the thermocline (dots), the WTD indicator for the minimum temperature difference (circles), and the mean values of climate variables, from 100 runs of Monte Carlo simulations (2001 - 2008 period). The wind speed and air temperature have the most significant impact on the stability of stratification.

Figures 2.13 and 2.13 compare the stability measures before and after the putative mixing event of 2008. The second figure excludes the extreme results from mixing in 2008. Although 68 out of 100 simulations that were run for the time period between 2001 and 2016 displayed mixing

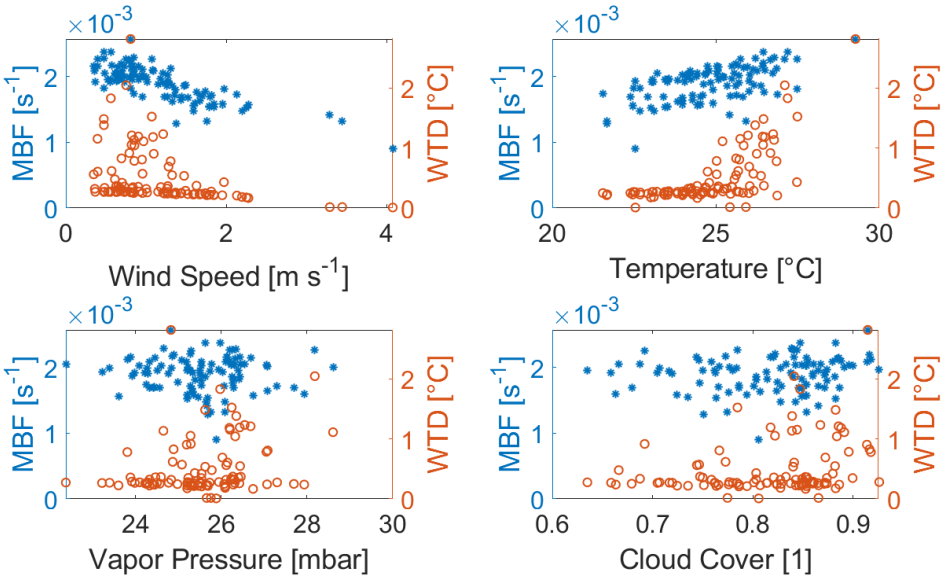

Figure 2.14: Correlation between MBF (dots), WTD (circles), and the mean values of climate variables, from 100 runs of Monte Carlo simulations (2009 - 2016 period). Notice that a lot of simulations' WTD between 2009 - 2016 period is non-zero.

(zero temperature gradient at some point during the simulation), almost all of these instances occurred prior to 2008. Only three out of 68 simulation runs had mixing after 2009 (Fig. 2.13, 2.14, 2.15). Prior to the strong climatic event in 2008 that promoted most vigorous mixing, the stability of the lake was weaker (Fig. 2.8). After that, the stability of Lake Towuti increased, which made subsequent mixing events more difficult due to increased density gradient resulting from cooler bottom water similar to the results seen in Fig. 2.2 and 2.8.

Fig. 2.15 illustrates the differences between these two different time ranges (before and after 2008), as reflected in each of our two stability measures. The WTD values plot above the 1:1 line, which indicates weaker temperature differences during the dry season (more prone to mixing) before 2008 than after 2009. The MBF values generally plot below the 1:1 line, indicating that the wet seasons before 2008 were somehow more conducive to stronger thermoclines.

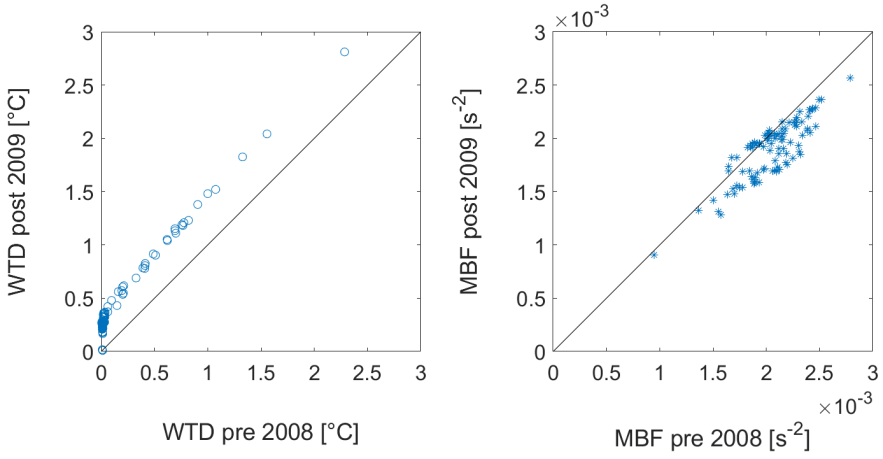

Figure 2.15: WTD and MBF indicator comparison between pre 2008 and post 2009 from simulation. With criteria of WTD $<$ 0.4 °C indicating mixing, there are 68 simulations simulated mixing before 2008, but only 3 of them also simulated mixing between 2009 - 2016

2.2.3 Lake Towuti during the Last Glacial Maximum

Simulations of Lake Towuti stratification under the hypothesized climatic conditions of the Last Glacial Maximum (LGM) show that lowering of the lake level, combined with colder and drier conditions, changes the stratification dynamics (Fig. 2.16). In a shallower lake, turbulence from the interactions of currents with the lake bottom may increase the mixing rates in the interior of the water column. Simulations suggest, however, that under the modern climate conditions lowering the lake level alone would not significantly influence the whole water temperature and the thermocline depth. As the lake level varied from 200 m to 100 m in the model, under the modern climate conditions, the temperature at the surface and the thermocline depth did not change significantly (Fig. 2.16 left column). The surface processes were still isolated from the bottom water. However, under the LGM climate conditions, which produced stronger negative heat fluxes at the surface, lowering lake level to 150 m resulted in a whole water column mixing almost every year (Fig. 2.16 right column). Lowering lake level also increased surface

temperatures and maximum thermocline depths during wet seasons under the LGM climate condition. The difference between the air temperature and the surface water temperature is kept at four °C under both the modern and the LGM climate.

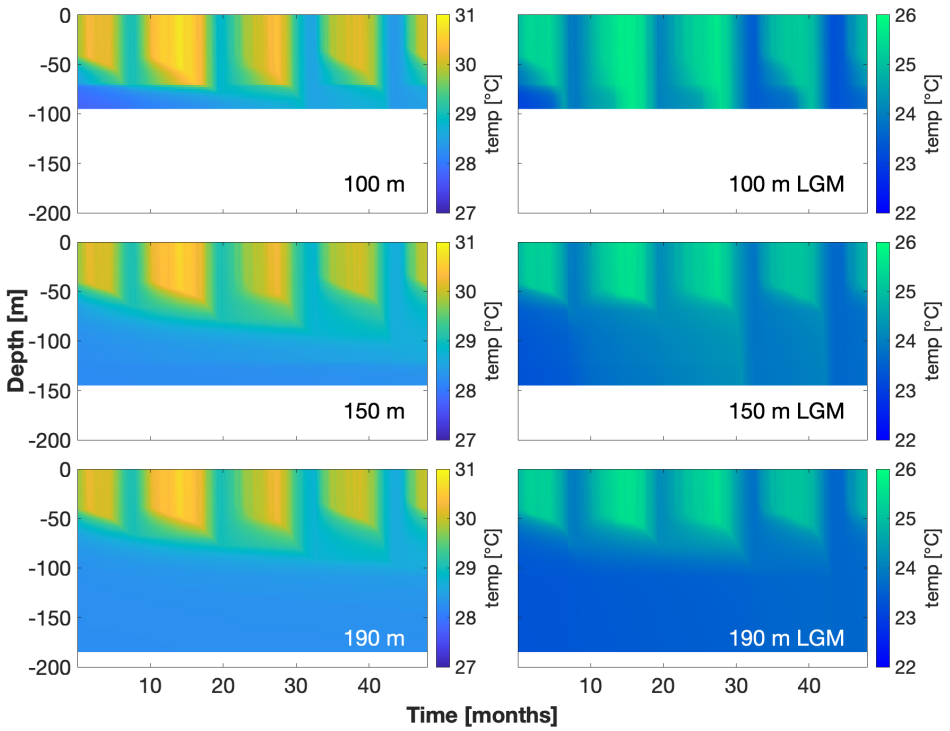

Figure 2.16: Simstrat simulation exploring conditions during the Last Glacial Maximum (LGM) for different water levels (100 m, 150 m, and 190 m) and for different climate conditions (left column : current ERA5 reanalysis climate conditions, right column : LGM climate conditions described in subsection 2.1.6). The simulated processes are similar to the nominal hydrodynamic simulation for the modern lake, but the outputs are cropped so that it represents a relatively steady stage of establishing LGM hydrodynamics.

2.3 Discussion

2.3.1 Multi-year Stability and Potential Oligomixis of Lake Towuti

Contrary to current beliefs about the meromixis in the lake, Lake Towuti may experience whole-water column mixing, i.e. it may be oligomictic rather than meromictic. The mixing in Lake Towuti, as in other similar tropical lakes, is mostly induced by strong, negative surface heat fluxes during the dry season. These heat fluxes continuously lower the mixolimnion temperature to that comparable to monimolimnion, until they induce mixing. Simulations, including sensitivity tests, show that the mixing regime of Lake Towuti may be borderline between meromixis and oligomixis. If Lake Towuti is truly oligomictic, mixing can be expected to happen about once a decade, at the times when the thermal gradient is weak and weather conditions are especially cold and dry. Mixing events are unlikely to be very frequent, as cooling of the bottom waters during mixing establishes a stronger temperature gradient in the following season, while diffusion of heat from the mixolimnion to reheat the monimolimnion takes several years (see below).

Our simulation (Fig. 2.4) suggests a possibility of a series of brief mixing events between 2000 and 2008. After a major mixing event in 2008, the bottom water cooled down significantly, setting up for increased stability thereafter. The lake was more stably stratified from 2009 onward.

Evidence for deep mixing also can be seen in the observational data. CTD profiles from 2000 to 2009 (Fig. 2.7) show more variability in deep water temperatures than could be explained if Lake Towuti were permanently stratified. In particular, temperature in the bottom water had decreased in 2009 compared to 2006 (Fig. 2.7). In the absence of intrusions of cold groundwater, this could only happen if the surface water cooled sufficiently to sink down into the monimolimnion.

After deep mixing, stratification reestablishes after receiving enough surface warming during the wet season. After restratification, the lake surface again becomes isolated from the lake bottom. This isolation, however, does not inhibit the gradual diffusion of heat into the monimolimnion. The overall picture of lakes' mixing-stratification dynamics is discussed below.

2.3.2 Mechanisms of Stratification and Mixing

Strength of Stratification

The strength of stratification in Lake Towuti can be characterized by the cumulative Schmidt Stability (SS) and cumulative heat content (HC). Fig. 2.17 illustrates the typical SS and HC profiles that were calculated based on available CTD and mooring data. During the wet season, cumulative SS increases from 0 at the surface to 5 $\mathrm{kJ\,m^{-2}}$ at around 100 m, to more than 10 $\mathrm{kJ\,m^{-2}}$ at the maximum mooring depth 150 m. During the dry season, the magnitude of SS is much smaller, at around 1 $\mathrm{kJ\,m^{-2}}$ at 150 m. The magnitude of cumulative SS indicates the mechanical energy required to homogenize the water column down to a given depth. During the wet season, cumulative HC is 0 at the surface, 4×10^5 $\mathrm{kJ\,m^{-2}}$ at the 100 m and 4.5×10^5 $\mathrm{kJ\,m^{-2}}$ at 150 m. The magnitude of cumulative HC indicates the negative thermal energy required to remove the heat and cool down all the water above the given depth.

We can compare these numbers, respectively, with the typical wind power and surface heat fluxes at Lake Towuti. The wind power per unit area being transferred into a lake ($P_{kin,W}$) can be estimated using the approximation of Imboden and Wüest (1995):

$$P_{kin,W} = \chi \rho_{air} C_{10} W_{10}^3 \tag{2.24}$$

Here, χ is the fraction of wind energy at 10 m above the surface being transferred into the

lake, typically 1–2%. ρ_{air} is the density of air, 1.2 $\mathrm{kg\,m^{-3}}$. C_{10} is the drag coefficient, which depends on the lake surface roughness. It is typically 0.001 for wind speed smaller than 7 $\mathrm{m\,s^{-1}}$ (Imboden and Wüest, 1995). Thus, for an average wind speed (10 m above surface, W_{10}) around 0.85 $\mathrm{m\,s^{-1}}$, the typical wind power transferred into the lake is around 1×10^{-5} $\mathrm{W\,m^{-2}}$. For a three-month season, the total wind energy is on the order of 0.1 $\mathrm{kJ\,m^{-2}}$. By comparing this value to a typical SS profile (Fig. 2.17), the mixing power induced by pure wind drag can only mix the water column down to about 30 meters in a three month season.

Lake Towuti's seasonal heat fluxes simulated by Simstrat are shown in Fig. 2.9. The net surface heat flux varies between -150 $\mathrm{W\,m^{-2}}$ from June to September to +150 $\mathrm{W\,m^{-2}}$ from September to January. The negative (positive) heat fluxes during the dry (wet) season is on the order of 1×10^5–1×10^6 $\mathrm{kJ\,m^{-2}}$. The annual heat imbalance is on the order of $1 \times 10^5 \mathrm{kJ\,m^{-2}}$. Comparison with the HC in Fig. 2.17 shows that such heat fluxes are capable of extending mixing substantially downward into the monimolimnion during the dry season, potentially even to the lake bottom in more extreme conditions.

Thus, variations in heat fluxes are the major mechanism for stabilizing and destabilizing the water column. Mixing induced by direct wind turbulent energy is limited in comparison, as is commonly recognized (Imboden and Wüest, 1995). While these numbers serve as a simple illustration of the relative importance of mechanical and thermal energies (Imboden and Wüest, 1995), the processes that distribute both mechanical and thermal energies throughout the lake and their associated time scales are also important. They include seiche activities, turbulent energy dissipation, and non-linear variations in temperature being an active tracer.

Heat Diffusion

Even a strongly stratified water column would not stop the exchanges of heat and substances between the surface and bottom layers. The dominant transport process is diffusion. Molecular

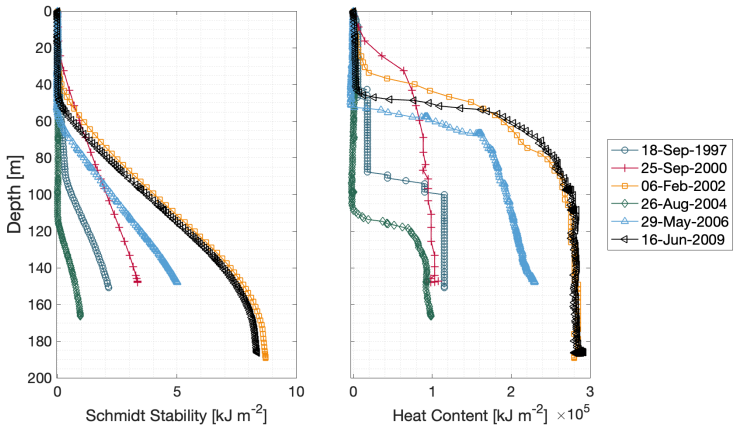

(a) Cumulative stability (SS) and heat content (HC) calculated based on CTD data.

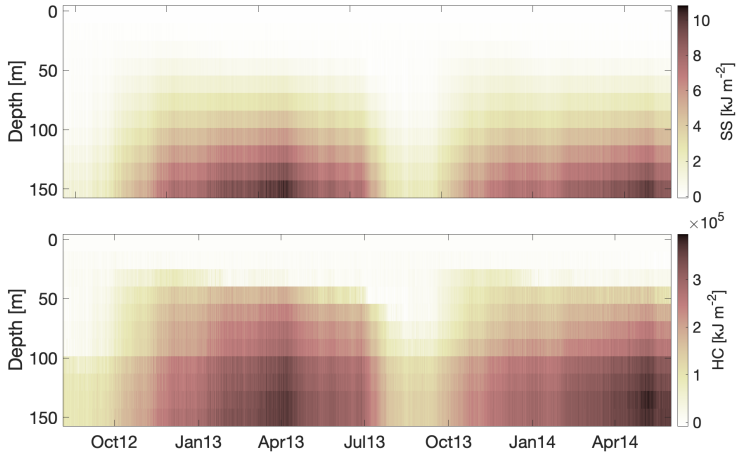

(b) Cumulative SS and HC calculated from mooring data

Figure 2.17: Schmidt Stability and Heat Content (relative to the water temperature at the calculated depth). The magnitude of SS indicates the mechanical energy required to homogenize the water column to the desired depth while the magnitude of HC indicates the negative thermal energy required to cool down all the water above that depth.

diffusivity (commonly 1×10^{-9} $m^2\,s^{-1}$) is usually too slow to significantly affect the molecule concentration profiles in stagnant water columns. The diffusivity of heat has a greater magnitude (commonly 1×10^{-6} $m^2\,s^{-1}$). The turbulent diffusion, even during the stratified season in Lake Towuti (1×10^{-6} $m^2\,s^{-1}$), in contrast, increases the magnitude of vertical diffusivity for both

chemicals and heat.

The depth and time scales for the diffusion process in the monimolimnion can be estimated by a back-of-the-envelope calculation using the Einstein's equation for Brownian motion:

$$\bar{x^2} = 2Dt \tag{2.25}$$

The turbulent diffusivity under stratified conditions in Lake Towuti is D $\approx 1 \times 10^{-6}$ m^2 s^{-1} (Fig. 3.1). Under this rate of diffusion, heat can be transported 60 meter downwards within a year:

$$x_{max} = \sqrt{2 * 10^{-6} m^2 s^{-1} * 31536000 s} \approx 60 m \tag{2.26}$$

This process can gradually warm up the monimolimnion temperature, and reduce the temperature difference between the lake's surface and bottom. The time scale for this diffusional process to restore pre-mixing temperature gradient can be estimated:

$$\begin{aligned} \frac{\Delta T}{\Delta t} &\approx K_z \frac{\Delta T}{\Delta z} \\ \Delta t &\approx 0.5^{\circ}\mathrm{C} / (1 \times 10^{-6} \mathrm{m^2\,s^{-1}} \frac{1^{\circ}\mathrm{C}}{(20\ m)^2}) \\ &\approx 1 \times 10^8\ seconds \approx 3\ years \end{aligned} \tag{2.27}$$

This diffusional process transports heat into the monimolimnion. However, because the surface water temperature is balanced with the surface atmospheric conditions at a much faster rate, the state of the mixolimnion does not experience drastic changes in its average temperature. Once the mixolimnion supplies heat to warm up the monimolimnion, the balance between mixolimnion and surface weather condition will restore the surface water temperature, via

decreased negative fluxes of blackbody radiation, sensible and latent heat. These processes keep mixolimnion warm as usual, without being significantly disturbed by the cold monimolimnion. Increasing global average air temperature might further warm up the surface temperature, whose effect will be discussed in detail later.

The Effect of Precipitation

The momentum and heat effect of the precipitation is not simulated in Simstrat. However, a back-of-envelope calculation suggests that the effect of surface precipitation is small. The heat content (per unit area) of the precipitation (reference to 28 °C) in one hour, 5 mm/h rainfall event is:

$$\begin{aligned} HC/Area &= \rho_w \times rainfallDepth \times c_p \times \Delta T \\ &= 996\ \mathrm{kg\,m^{-3}} \times 5 \times 10^{-3}\ \mathrm{m} \times 4189\ \mathrm{J\,°C^{-1}\,kg^{-1}} \times (21-28)\ \mathrm{°C} \\ &= -1.46 \times 10^{5}\ \mathrm{J\,m^{-2}} \\ &= -1.46 \times 10^{2}\ \mathrm{kJ\,m^{-2}} \end{aligned} \tag{2.28}$$

Compared to the value magnitude of heat content plot in Fig. 2.17, the cooling power of the one-hour precipitation is not strong enough to destroy a stable thermocline unless the precipitation is 100 to 1000 fold greater than 5 mm/hr or it lasts for a much longer time (100 to 1000 hours).

Stratification Mechanism

The stability of Lake Towuti is determined by the temperature gradient, as the salinity is very low (conductivity of 140 - 195 $\mu\mathrm{S\,cm^{-1}}$ is equivalent to salinity 1.4×10^{-5}–$1.9 \times 10^{-5}\ \mathrm{g\,kg^{-1}}$) and has only a weak gradient. In the absence of a salinity gradient, the water temperature gradient plays a key role in the stratification and mixing of Lake Towuti.

Seasonal climate patterns are the main cause of the variations in water temperature, and thus, lake stability. Wet seasons come with higher air temperature, lower wind speed, higher vapor pressure, and higher cloud cover, resulting in positive surface heat flux. This increases the heat content in the lake's epilimnion and establishes stronger stratification. The opposite happens in the dry season, when air temperature decreases, wind speed increases, and humidity and cloud cover decreases, leading to negative surface heat flux. This process cools down the lake surface, reduces the overall temperature gradient, induces mixolimnion mixing, and destabilizes the lake.

Mixolimnion mixing almost always starts in the dry season, when naturally the negative heat flux cools down the surface. During extreme climate events, mixing can extend to the whole water column. Over the multi-year time scale, air temperature influences lake stability the most. Average air temperatures below 24 °C would result in mixing during the simulated period (2000 - 2016). Wind speed has the potential to destabilize the water column as well, but at more extreme values. In Lake Towuti, if the average wind speed is greater than 2 $\mathrm{m\,s^{-1}}$ (double of current wind speed), the lake is likely to mix. Wind affects the stability by both mechanical and thermal effects, as higher wind decreases heat fluxes and induces instability.

Besides immediate climate variations over the lake, lake history also plays an important role in how the lake reacts to changes in climate. Climate variables influence the heat flux at the surface of the lake. A negative heat flux would only lead to mixing when it is sufficient to cool down the whole mixolimnion temperature to that being comparable to monimolimnion. If mixolimnion is deeper and warmer, or when monimolimnion is much cooler, it will need more sustained and stronger negative heat flux to cool down the lake's surface and induce whole water column mixing.

Interaction between meteorological variations and lake history create a negative feedback loop (Fig. 2.18). Full water column mixing reduces the temperature both at the lake's surface and

bottom. The overall heat content and Schmidt stability decrease. After the event, bottom water continues to stay cold, while the surface temperature increases. The surface heat flux plays an important role in regulating the surface temperature so that it reaches an equilibrium dictated by surface air temperature and other weather conditions. The reestablished surface temperature accompanied by cooled bottom water leads to an increase in surface and bottom temperature difference. The greater difference leads to an increase in Schmidt Stability and makes the lake more resistant to mixing. Thus, even with similar magnitudes of climate variability, Lake Towuti is less likely to be mixed again after 2008, when a major mixing and cooling happens. The strong stratification, however, will not prohibit heat exchange between the surface and the bottom part of the lake. This process is accomplished by heat diffusion ($\approx$ 60 m/yr). This divisional process warms up lake bottom temperature, and reduces the overall stratification strength gradually. Overtime, the lake goes back to its original state where surface and bottom temperature difference and lake stability are weak. The overall process resembles a negative feedback cycle.

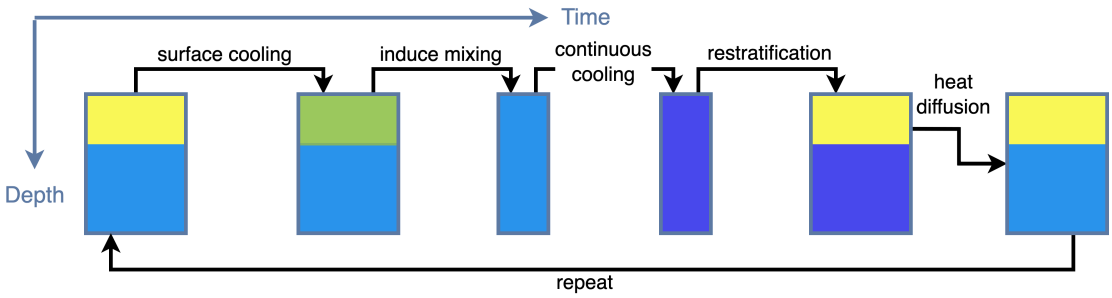

Figure 2.18: Conceptual diagram of the mixing-stratification dynamics in Lake Towuti. Starting from a weak thermal gradient, when there is a strong negative surface heat flux, surface water cools down to a point where the whole water column mixes. If the negative heat flux is strong, the whole lake cools down by a significant amount. After this event, the lake gradually reestablishes its surface temperature, while the bottom water stays cold. Lake stability after restratification gets stronger, and thus the lake is less vulnerable to mixing. With enough time, the gradual diffusional process will blend out this strong stratification, and make it weak again, to its original state.

2.3.3 Lake Towuti During the Last Glacial Maximum

The cooler and drier condition during the LGM affects the stratification of Lake Towuti by reducing the lake level, and reducing the surface heat flux. Hydrodynamic simulation applying LGM climate and various water depths indicates that the lake level of Towuti being 150 meter or less can lead to frequent whole water column mixing. This ties to the oxidized water column conditions proposed by Russell et al. (2020).

An interesting phenomenon is observed with the LGM simulations. Varying lake level did not result in significant difference in lake temperature structure under modern climate conditions. However, under LGM climate conditions, the lowering of lake level increases thermocline depth, and increases overall heat content. This is because shallower lake during LGM had higher turbulent diffusivity, significantly increasing the rate of heat diffusion, allowing faster penetration of surface heat towards the bottom. The overall surface heat flux will adjust to this increase, and leads to the increase in overall heat content.

2.3.4 The Impact of Global Climate Changes

The effect of climate on stratification of tropical lakes is often invoked in discussions but rarely quantified in mechanistic terms. In the context of climate warming, stratification of lakes is believed to strengthen globally (Woolway and Merchant, 2019) as warming of the surface increases the temperature difference from the deeper waters.

The global average air temperature has increased, on average, by 0.6 °C over the 20th century (Albritton et al., 2001). The effect of the warming trend has been seen on global lakes. The increase in surface water temperature on Lake Kivu has been estimated to be 0.12 °C per decade (Katsev et al., 2014). The warming rate of Lake Superior summer temperature is 0.35 °C per decade Austin and Colman (2008). From two-decades of simulations conducted in Lake Towuti, however, the warming trend is not yet significant and it is difficult to be separated from the rest

of yearly variabilities.

From previous discussions, air temperature is recognized as the major control on surface lake temperature and lake stability. Based on this conclusion, it is foreseeable that Lake Towuti, and similar tropical lakes will experience increasing lake surface temperature and increase stability under warming air temperature. The negative feedback proposed in Fig. 2.18 might still be in effect if the rate of increasing air temperature does not exceed the rate of restoring temperature gradient via heat diffusion. This feedback, however, will not prevent the warming of a lake's overall temperature. Detailed investigation is still needed to distinguish the patterns of climate change during dry season versus during wet season, as the timing of the changes is important in dictating if a lake will be fully mixed.

2.3.5 Correlation with ENSO

Located in the center of the Indo-Pacific warm pool (IPWP), Sulawesi Island is expected to be influenced by decadal climate variations, including El Niño–Southern Oscillation (ENSO). In the tropical western Pacific region, El Niño years often correspond to a drier climate with lower precipitation (Xie et al., 2016). The common conception is that, the cooler and drier climate conditions during El Niño years will favor the mixing of the lake.

The correlation, however, is not typically strong concluded from the simulation. The mixing event in 2002-2003 coincided with an El Niño year while the 2008-2009 mixing event coincided with a La Niña year (Fig. 2.11). This could be because the correlation between ENSO index and Indonesia local climate is not straightforward as well. Most climate studies have focused on the effect of ENSO events on rainfall over Indonesia, and obtained somewhat satisfactory correlations with regional variations (As-syakur et al., 2014, Supari et al., 2018, Firmansyah et al., 2022). However, there are limited investigations on air temperature and wind speed. The correlation between ENSO MEI.v2 index and ERA5 reanalysis meteorology over Lake Towuti

is looked at in more detail in appendix (Fig. D.4). Generally, the correlation is weak.

This weak correlation revealed the complexity of the ENSO system, since it was developed to characterize the global multi-decadal climate cycle. Investigations on sea surface temperature with the regional climate system, such as the Indo-Pacific Warm Pool (IPWP), might yield stronger correlations and provide relevant knowledge about the lake stability under the influence of climatic variabilities.

Besides the weak correlation between the ENSO index and local climate, the lack of correspondence could be due to the fact that the stratification is also affected by the history of the lake. Stability and heat content from previous seasons and years contribute to how the lake responds to immediate weather conditions.

2.3.6 What Makes a Tropical Lake Meromictic

From the inspection on Lake Towuti dynamics, a general conclusion is given for tropical lakes. Tropical lakes have very different climate cycles compared to mid or high latitude lakes. The seasonality over the tropics is often classified into dry-wet seasons. However, compared to mid-latitude lakes, the water temperature in tropical lakes rarely goes through drastic changes annually. This provides the basis for tropical lakes to stay stably stratified.

For thermogenic tropical lakes, their stratification is mainly maintained by an often weak temperature gradient between the surface and bottom water. They lack other stability mechanisms since the salinity content is not pronounced. Thus, these lakes can be heavily impacted by the changes of the surrounding climate. An episode of strong, negative heat flux, induced by cooler and drier climate can disrupt this thermal stratification. The effect of heat flux is related to the lake's previous history. When the lake originally had a cold monimolimnion, or a warmer and thicker mixolimnion, it takes greater effort for these negative surface heat flux to cool down the lake's surface and induce mixing.

Other properties of these lakes can affect how they respond to the changes in climate and surface heat flux. A lake's morphology plays a vital role. Deeper equatorial lakes with smaller surface area protects the lake from variations in surface climate conditions. The maximum depth is especially important (confirming the results observed from Kraemer et al. (2015)). As Katsev et al. (2017) point out, some typical tropical thermogenic lake (Lake Malawi, Tanganyika, and Matano) have seasonal thermocline depth at 30-40 m during wet season, and 80-100 m during dry season. Based on this estimation, one can expect that tropical lakes that are less than 100 m deep are likely to be mixed annually. Tropical lakes that are 100 - 200 m deep, such as Lake Towuti, are more stable, but still likely to be mixed occasionally. Deeper tropical lakes, such as Lake Tanganyika, Malawi, and Matano, have greater probability of staying meromictic for centuries. Lake Atitlan and Lake Toba, for example, for which long term monitoring data are lacking, are likely to stay meromictic because their maximum depths are greater than 200 m.

The simple categorization based on lake depth is not definitive. Variations can be induced by several other factors as well. Firstly, it depends on the details of the tropical climate where the lake is based. Tropical lakes at higher latitude have stronger seasonal cycles that amplifies the effect of negative surface heat flux during dry seasons. Additionally, lake trophic status and light attenuation rate strongly control thermocline depth based on their effect on absorption of solar radiation. Heiskanen et al. (2015) has pointed out the importance of water clarity on their response to climate change. Eutrophic lakes often have stronger abilities to scatter light, resulting in larger lake attenuation coefficient. Thus, the solar radiation absorption throughout the water column will attenuate faster, leading to warmer and shallower epilimnion. These lakes will be less susceptible to mixing.

2.3.7 Performance of the Model, Caveats of Interpretations

Overall, Simstrat forced by ERA5 reanalysis hourly climate matches the observational temperature range and stratification patterns. The simulated temperature profiles are within 1 °C difference from all the observational profiles. Simulated profiles also match the pattern of temporal progression of discrete CTD prior to 2009 and continuous mooring between 2012 and 2015.

However, there are few limitations from the hydrodynamic simulations in this project. (1) Simstrat simulates mixing processes by imposing larger turbulence diffusion terms (ν terms, related to turbulent kinetic energy and dissipation, proportional to $\frac{k^2}{\varepsilon}$), rather than including the physical advection process. (2) Simstrat assumes 1-D physics. Depending on where the CTD and mooring data are measured in Lake Towuti, the observed temperature may indicate a slightly different physical setting than what was modeled. The limitation of 1-D model also includes the empirical simulations of seiche activities, which could be better modeled with two or three-dimensional models. This was not helped by the fact that these empirical seiche parameters are not calibrated in Lake Towuti due to its limited mooring data. (3) There are no direct measurements of meteorology at the lake's surface. Thus, the climate forcing inputs are only available with reanalysis datasets. Available weather stations are far away from Lake Towuti and are at lower altitudes. They cannot provide confident verification. (4) There are other limitations in input data. Such as, there is no information on hydrological inputs, and no information on light attenuation variability. Thus, they are assumed to be reasonable constants. This might result in simulations deviating from real life values.

2.4 Conclusions

Using hydrodynamic model simulation, it is revealed that Lake Towuti has possibly been completely mixed at least once in the 2000s. The mixing is induced largely by cooler air during the dry season, when the lake has weak stability. The major mixing event cools down the bottom water temperature, resulting in an enlarged temperature difference once the lake restratifies again during wet season. It increases lake stability thereafter. This process can be described by a negative feedback loop (Fig. 2.18).

Since the maximum seasonal thermocline depth for global major thermogenic meromictic tropical lakes is around 80 m, we concluded a bathymetry division that determines if a tropical lake (without salinity gradient) is going to be meromictic. The criteria is:

Maximum Depth	Mixing status
$<$ 100 m	warm monomictic
100 m - 200 m	oligomictic
$>$ 200 m	meromictic

Table 2.4: Concluded mixing criteria for tropical lakes without salinity gradient

Of course, this criteria fluctuates with the climate conditions and trophic levels. When the climate is cooler, drier, and windier, the lakes are more susceptible to mixing. When a lake is more eutrophic, resulting in faster light attenuation and shallower thermocline, it is less prone to mixing.

The climate during the LGM was colder and drier. Thus, tropical lakes during that time were prone to mixing. The cooler and drier conditions also resulted in reduced lake levels. For Lake Towuti, we suggest it would frequently mix during the LGM if it were less than 150 meter deep, setting the environmental conditions for frequent oxygenation.

Chapter 3

Biogeochemical Model

3.1 Introduction

This chapter explores the chemical dynamics in Lake Towuti, in particular the effects of changes in physical stratification on the distributions of redox-sensitive chemical species: oxygen, sulfate/sulfide, iron(II)/(III), and methane. It approaches this problem with the help of a reaction-transport biogeochemical model.

The model simulates the rates at which the chemicals accumulate or become depleted in the lake's monimolimnion. The results should inform us about the timescales of stratification or mixing that are required for the observed (Fig. 3.3 dot profiles, provided by Dr. Sean Crowe) chemical concentrations. When stratification persists for a long time, oxygen eventually becomes depleted. Anoxic environments favor reduced species (H_2S, Fe^{2+}, and CH_4). Mixing of the entire water-column, in contrast, reintroduces oxygen into the deep waters and can reset the concentrations of these reduced species. An agreement between the observations and the distributions of O_2, H_2S and Fe^{2+} simulated under the conditions of a persistent stable stratification would imply that no mixing happened in the recent past. Otherwise, deviations

in the concentrations of reduced species might indicate a possible non-steady state, e.g. after an episodic mixing. Numerical simulations may then provide estimates for the time scales involved.

To investigate whether the chemical dynamics in Lake Towuti may be used as an independent way of verifying the findings from the previous chapter about the possibility of episodic mixing, we are seeking answers to the following questions:

1. How long does it take to deplete oxygen in the lake bottom waters when the lake becomes stably stratified after a complete mixing?
2. How quickly can oxygen be replenished, and to what concentrations, during the episodes of weak mixing, such as during the potential seasonal events that are predicted by our hydrodynamic model?
3. How do the dynamics of stratification and mixing affect the redox chemistry in the monimolimnion? In particular, how do the concentrations of dissolved ferrous iron and dissolved hydrogen sulfide vary with time after the oxygenation events, and following the restoration of anoxic conditions?

3.2 Methodology

3.2.1 Chemistry Model

We used a one-dimensional reaction-transport biogeochemical model. The model considers the kinetics of biogeochemical reactions together with the physical transport of the reactants and products by turbulent diffusion. It features an explicit treatment of microbial biomasses that catalyze the anaerobic processes of iron reduction, sulfate reduction, and methanogenesis through the respective microbial metabolisms. The model was adopted from Sergei Katsev and Itay Halevy (PNAS in prep) and its description is given in Appendix C. The model solves a

system of partial differential equations for the set of included chemical species. The dominant equation describing the dynamics of chemical species is:

$$\frac{\partial C_j}{\partial t} = \frac{\partial}{\partial z}\left(K_z(z)\frac{\partial C_j}{\partial z}\right) - v_j\frac{\partial C_j}{\partial z} + \sum_i \nu_i R_{ij} \tag{3.1}$$

Here, z is the depth below the lake surface, K_z is the depth-dependent vertical diffusion coefficient, C_j is the concentration of a chemical species, v_j is the advection (or settling, for solid particles) velocity, and R_{ij} are the rates of reactions related to the chemical species with stoichiometric coefficients ν_i. The reactions involved in this model describe the transformations of oxygen, carbon, sulfur, and iron (Table C.2). Table C.3 and C.4 describe the corresponding kinetic formulations and parameter values. The model was supplied with parameters that were the best estimates for the conditions in Lake Towuti.

3.2.2 Using the K_z from the Hydrodynamic Model

To describe the intensity of physical transport within the stratified water column, the chemical model uses the K_z profile that is approximated based on the results from the hydrodynamic model described in the previous chapter. As described above, the $k-\varepsilon$ model Simstrat simulates mixing as a diffusive process using molecular and turbulent eddy diffusivity. Advection or convection of water, which are rare under stratified conditions, are not explicitly modeled but rather approximated by roughly equivalent increases in eddy diffusivity. The turbulent diffusivity of temperature from the model output is thought to be a good representation for the transport (K_z) of chemical species in the chemistry model, as both temperature and solutes are distributed by turbulent eddies, at rates typically above the molecular diffusion of heat and well above the molecular diffusion of solutes. The v_j term in Eq. 3.1 only applies to solid chemical species, describing their downward settling.

The temporal evolution of K_z in Lake Towuti simulated by the hydrodynamic model is shown in Fig. 3.1. Imposing this fully time-resolved evolution of K_z on the chemical model has proved to be computationally challenging, however. Rather, to answer questions about the time scales of the chemical dynamics formulated above, we considered two contrasting (simpler) scenarios for the temporal variations in K_z. One (the "stable stratification" scenario) describes a typical, time-averaged, K_z profile during a prolonged stratification period. The values for this scenario were extracted from the 2003 dry and wet seasons. The other (the "mixing" scenario) uses the K_z profile that characterizes the brief period of enhanced mixing, such as during the 2008 hypothesized mixing event. The values of K_z for this scenario were extracted from the 2008 dry season. As the sharp variations in K_z by several orders of magnitude across a narrow thermocline generate excessive stiffness in the MATLAB pdepe solver, we further simplified the profile in chemical simulations by using its analytical approximation, as illustrated in Fig. 3.2. The analytical profile was constructed using Eq.3.2:

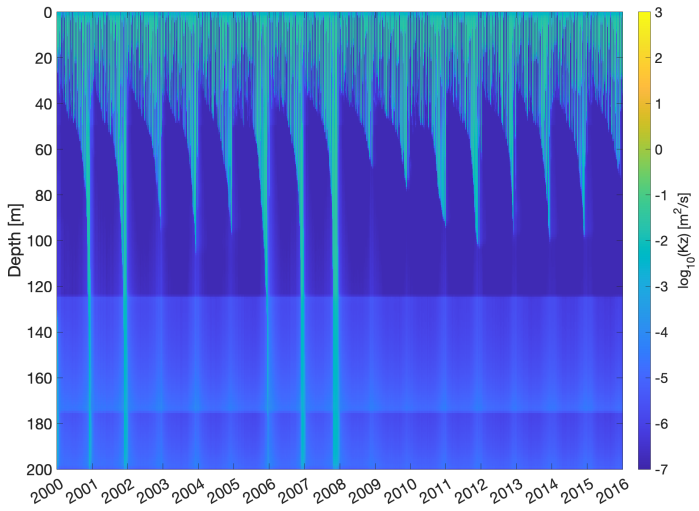

Figure 3.1: Turbulent diffusivity of temperature, equivalent to K_z, simulated by the hydrodynamic model discussed in Chapter 2

$$K_z(z) = K_z^0 \left(f_{Kz} + \frac{1 - f_{Kz}}{1 + e^{(z-H_K)/h_K}} \right) + 3(\frac{z}{60})^4 \tag{3.2}$$

Here K_z^0 is the surface diffusivity, f_{Kz} is the fraction of the bottom diffusivity in relation to the surface. H_k is the width of thermocline, and h_k is the thermocline depth for mixing. The parameters used to simulate a typical stratify or mixing K_z are listed in Table 3.1. The results are visualized in Fig. 3.2.

	stratify	mix scenario 1	mix scenario 2	units
K_z^0	3×10^{-4}	3×10^{-3}	1×10^{-2}	$m^2\,s^{-1}$
f_{Kz}	1×10^{-3}	1×10^{-1}	1×10^{-1}	$m^2\,s^{-1}$
H_k	8	8	8	m
h_k	40	40	40	m

Table 3.1: Parameters defining analytical K_z profiles

The analytical K_z was approximated based on the typical variations, tailored to the resolution of the PDEs in MATLAB. While the analytical profile for the "steady state" scenario has a more diffused thermocline than the profiles obtained in the simulation (Fig. 3.2), the wider "effective" width of the thermocline does reflect the vertical range within which the thermocline migrates seasonally in Lake Towuti. Key to the downward transport of oxygen and the accumulation of reduced species is the minimum value of K_z within the thermocline, as it is that minimum value that limits the vertical transport of substances between the surface and deep waters. The minimum value in the analytical profile is somewhat higher than minima in the individual simulated profiles (Fig. 3.2), but reflects the potential influences of the brief periods of incomplete mixing during the dry season, when K_z in the thermocline region increases by up to two orders of magnitude (Fig. 3.1). The lower values of K_z in the epilimnion compared to the simulated values do not have a significant effect, as mixing in the epilimnion is still vigorous enough to effectively transport substances across the surface mixed layer.

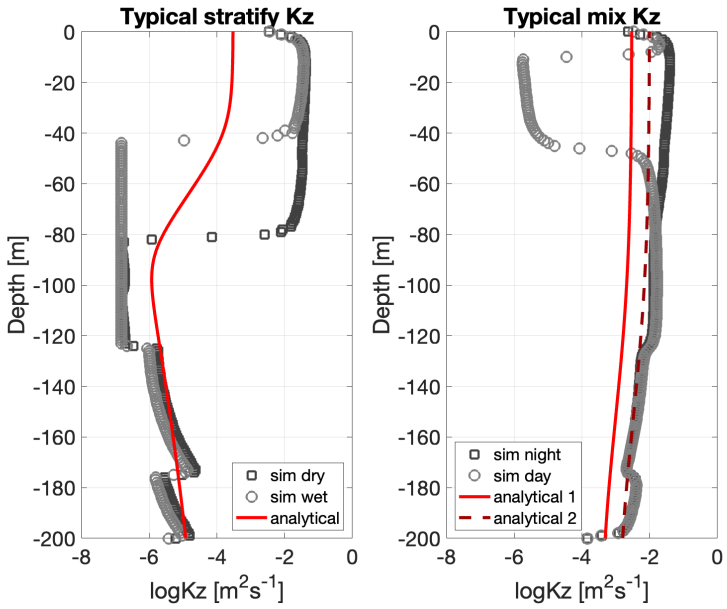

Figure 3.2: Typical stratification (left) and mixing (right) K_z profiles extracted from the hydrodynamic model (square and circular markers) and their corresponding analytical approximation (solid line) used in the biogeochemical model.

3.2.3 Simulation Procedure

The K_z profiles described above were treated within individual simulation runs as constant profiles, without temporal dynamics. In order to mimic the dynamic changes in K_z, separate simulation runs were performed, based on the following procedures:

1. Obtaining long-term stratification with bottom-water anoxia: Starting from oxic initial conditions, the ”stable stratification” K_z profile was applied for 40 years, which was sufficient for the bottom water to become anoxic for ten years and for reduced chemical species to accumulate.

2. Simulating brief periods of enhanced mixing: Starting from anoxic initial conditions, the mixing K_z profile was applied and the simulation was run for 2 months (which was the characteristic mixing duration observed from the hydrodynamic model).

3. Simulating recovery of stratification after a brief mixing event: Starting from profiles after the mixing event, the stratified K_z profile was applied again for seven years.

The obtained temporal evolution of the chemical profiles, recorded at regular time periods, were then inspected, looking for the characteristic time scales over which the reduced chemicals (particularly H_2S and Fe^{2+}) reached concentrations similar to their observed magnitudes.

3.3 Results

Starting from fully oxygenated condition, oxygen becomes depleted below 120 m after about 30 years of steady stratification (Fig. 3.3), causing accumulation of H_2S, Fe^{2+} and CH_4. Sulfate (SO_4) reduction decreases sulfate concentration below the oxycline but does not deplete it completely, in agreement with observations and in contrast to Lake Matano (Crowe et al., 2011). Sulfate is reduced into hydrogen sulfide, which could be oxicized by Fe(III) and precipitate out as elemental sulfur. This process reduces overall sulfate + sulfide concentration within the water column, especially after year 40, when highly reactive Fe(III) being produced by oxidizing Fe^{2+} at oxycline reacts with sulfide and remove it from the water column. Hydrogen sulfide accumulates to low micro molar levels, also similar to observations. The shape of the sulfide profile achieved after 40 years of simulation time differs somewhat from the observations, with the simulated profile accumulating higher concentration of sulfide around the sulfate reduction zone. The H_2S concentration reaches its maximum levels within a few years of the onset of anoxia, whereas Fe^{2+} and CH_4 continue to build up. Simulation had numerical problems to continue after 40 years. However, extending the stratification beyond 40 years is expected to further decrease the concentration of H_2S and increase the Fe^{2+} concentrations to significantly higher levels.

Two months of mixing at the intensities suggested by the hydrodynamic model transport oxygen to deeper and previously anoxic waters. The resultant concentrations of oxygen in the monimolimnion, nevertheless, remain low. For the weaker mixing scenario, when the K_z ranges between 3×10^{-3} at the surface to 3×10^{-4} $m^2\,s^{-1}$ at the bottom, the mixing season fails to fully oxygenate the deeper part of the lake, allowing for some presence of reduced species there (Fig. 3.4a). For the stronger mixing scenario, when the K_z ranges between 1×10^{-2} at the surface to 1×10^{-3} $m^2\,s^{-1}$ at the bottom, oxygen increases to tens of $\mu mol\,L^{-1}$ at the bottom of the lake, which is roughly a quarter of oxygen saturation concentration. This downward

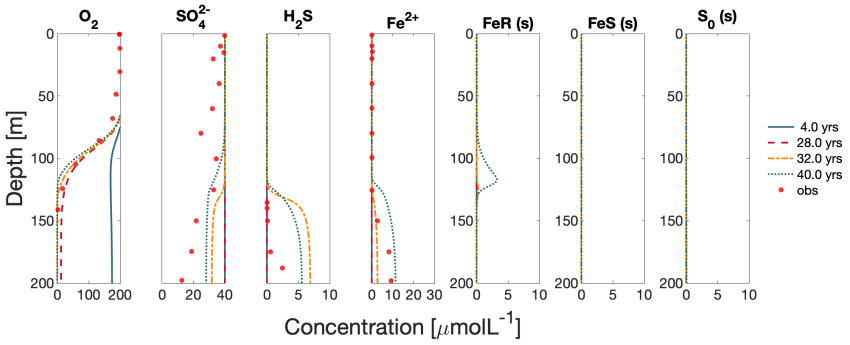

Figure 3.3: Development of chemical stratification starting from fully oxygenated initial condition. A typical "stratification" K_z was applied over the course of the entire simulation. Red circles are observational profiles (Dr. Sean Crowe, pers. comm.)

propagation of oxygen eliminates the reduced species (H_2S, Fe^{2+}, and CH_4) from the water column after about one month (Fig. 3.4b).

Resumption of stratification after brief and incomplete circulation restores the anoxia gradually. Following the weaker mixing scenario (Fig. 3.5a), H_2S slowly re-accumulates. The accumulation rate this time (2 $\mu mol\,L^{-1}$ in seven years of anoxia) is slower compared to when the anoxia was established after a prolonged stratification after fully oxic conditions (5 $\mu mol\,L^{-1}$ in 4 years of anoxia, Fig. 3.3). Fe^{2+} gradually accumulates as well, returning to its pre-mixing level at a rate comparable to the rate in Fig. 3.3. Following the stronger mixing scenario, however, oxygen persists in the deeper waters for several years and the reduced substances do not accumulate (Fig. 3.5b).

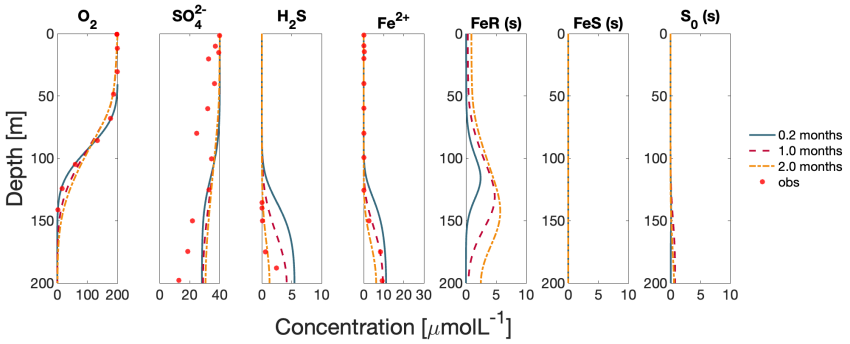

(a) The "weak mixing" scenario. Mixing K_z ranges from 3×10^{-3} to 3×10^{-4} $\mathrm{m\,s^{-2}}$

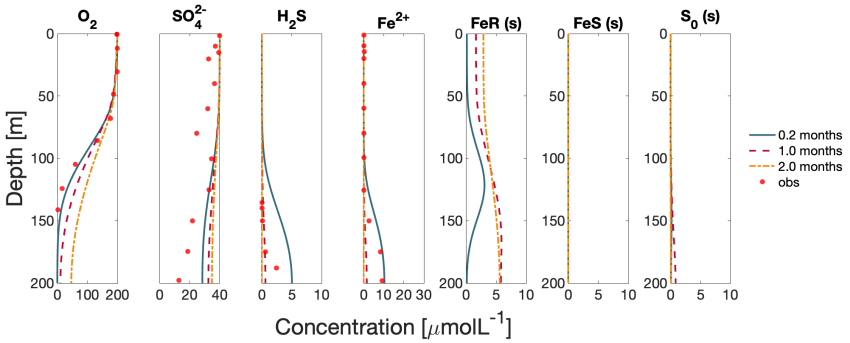

(b) The "strong mixing" scenario. Similar configuration as (a), but K_z ranges between 1×10^{-2} and 1×10^{-3} $\mathrm{m\,s^{-2}}$.

Figure 3.4: Chemical profiles during a mixing event. Starting from the initial conditions generated from the 40 years of stratification (Fig. 3.3), a typical mixing K_z was applied over the course of the simulation (2 months).

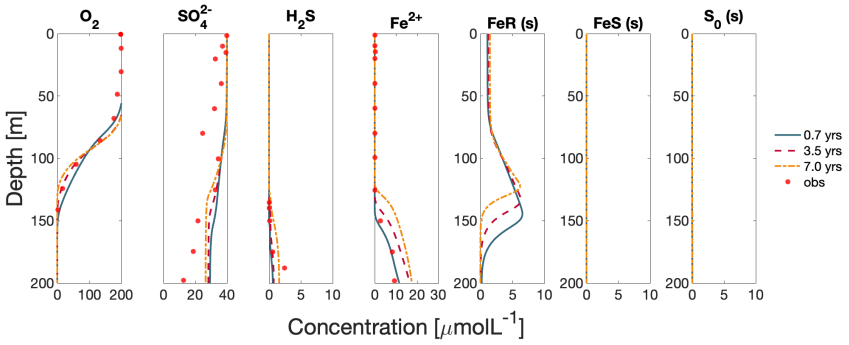

(a) Restratifying. Start from conditions after weak mixing (Figure 3.4a)

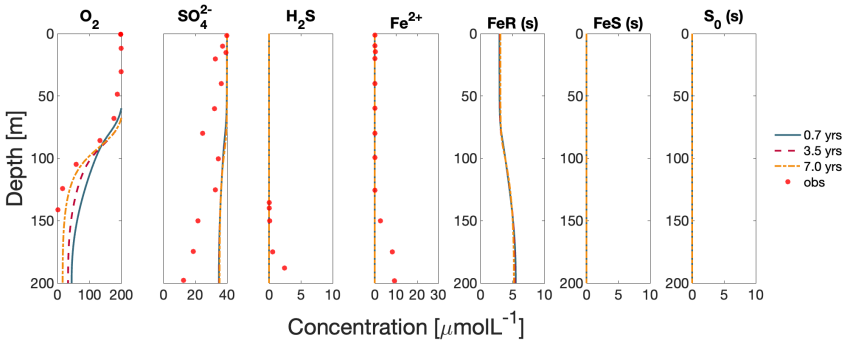

(b) Similar configuration as (a), but start from strong mixing (Figure 3.4b

Figure 3.5: Chemical profiles during the restratification process. Starting from conditions after mixing (Fig. 3.4), a typical stratify K_z was applied over the course of the simulation (seven years)

3.4 Discussion

3.4.1 Gentle Mixing Reproduces Observed Reduced Water Column

The simulations suggest that, in Lake Towuti, a fully oxygenated water column needs about thirty years of stratification to have oxygen depleted below the 120 m depth. Once oxygen is depleted, hydrogen sulfide and dissolved ferrous iron build up in the anoxic monimolimnion. When the H_2S and Fe^{2+} concentrations are both tens of $\mu mol l^{-1}$, the two aqueous species can coexist with respect to mineral FeS solubility (Rickard, 2006). Longer simulation could not be completed, for numerical reasons. However, interpreting from the trend of decreasing H_2S (by reactive Fe(III) oxidation) and continuously increasing Fe^{2+} (due to recycling of Fe^{2+} from sediments), it is suggested that Lake Towuti eventually favors ferruginous conditions.

The relatively stable balance of H_2S and Fe^{2+} in Lake Towuti is disturbed by introducing oxygen through mixing. The simulations suggest that the rate of oxygen introduction may be slower than one might envision in a turnover that would be analogous to the regular mixing of temperate lakes. Under the weak mixing scenario, the bottom part of the lake is not fully oxygenated within the two months of the mixing period. Even under a stronger mixing scenario where K_z is on the order of 1×10^{-3} to 1×10^{-2} $m^2 s^{-1}$, the bottom water does not bring enough oxygen to oxidize all the H_2S and Fe^{2+} in a month. The introduction of oxygen via turbulent mixing in the bottom water, however, generated reactive iron, which oxidized H_2S. The produced elemental sulfur S_0 then precipitated out and left the reaction zone. Restratification after this mixing does not reestablish the state observed when the anoxia was first established. The accumulation of H_2S is now slower, probably due to the suppression from reactive iron.

A ”strong mixing” event, even though it did not introduce oxygen to full saturation, was sufficient to deplete all the reduced species after one month. A seven-year restratification after the stronger mixing event was not sufficient to deplete oxygen and re-accumulate the reduced

species to the observed concentrations.

These results corroborate the findings from the hydrodynamic model and further challenge the hypothesis that Lake Towuti is permanently meromictic. If the lake had been stably stratified for more than 50 years without the introduction of oxygen via turbulent diffusivity, it is foreseeable that the anoxic condition would build up Fe^{2+} concentrations to hundreds $\mu mol\,L^{-1}$ level, similar to the level recorded in the neighboring Lake Matano Crowe et al. (2011). Lake Matano has Fe^{2+} concentrations around 140 $\mu mol\,L^{-1}$ in its lower strata, and only 0.3 $\mu mol\,L^{-1} H_2S$ within a narrow layer near the chemocline. Compared to Lake Matano, Lake Towuti has Fe^{2+} and H_2S concentrations of tens of $\mu mol\,L^{-1}$. This suggests that the chemistry of Lake Towuti is affected by periodic weak ventilation events, in contrast to Lake Matano that is permanently stratified.

3.4.2 Limitations of the Chemical Model

The uncertainties in the model could come from several sources. First, some of the model inputs and parameters are constrained within relatively wide ranges (Appendix B. For example, the surface flux of FeIII (F^0_{FeIII}), the recycling efficiency of reduced species in the sediment (f_{rec}), and the setting velocity of solid species (v_{settle}) are not measured directly for Lake Towuti but estimated, based on their likely realistic ranges. There are also uncertainties for chemical reaction rates that were established based on reaction kinetics typically observed in other environments and thermodynamics. Further, the time-independent analytical profiles for K_z, which differed from the hydrodynamic simulation outputs, could provide additional uncertainty. This chapter explored the upper and lower limits of K_z and suggested possible chemical dynamics in the lake. The model essentially simulates a one dimensional water column without areal extent. It only establishes boundary conditions at the surface and bottom, without considering the chemical exchanges that could happen at horizontal boundaries.

Adding some essential chemistry components can further support the interpretation of model outputs, but this was not achieved in this study. If we have more information about conservative irons (e.g. $[Cl^-]$), they can be used to calibrate or verify the transportation processes simulated by the chemistry model. Additionally, if we can add simulations about nutrient concentrations (e.g.$[PO_4{}^{3-}]$, $[NH_4{}^+]$), the model will provide more information regarding the effect of physical stratification on nutrient cycling and primary production.

3.5 Conclusion

The observed profiles of O_2, and $\mu mol\,L^{-1}$ levels of H_2S and Fe^{2+} coexisting in Lake Towuti can be reproduced by the model if stratification and anoxia persist for up to a decade. Short and weak mixing events could have happened between several months and several years prior to the measurements. The chemical profiles that were mostly taken in 2013 are thus consistent with the possibility of weak circulation and low-level oxygenation as a result of the 2008 weather anomaly. Anoxia longer than a decade would lead to further consumption of H_2S and accumulation of Fe^{2+} to levels above those observed, potentially to $\approx$ 100 uM as in Lake Matano.

Chapter 4

Conclusion

This project simulates the physics and chemistry of Lake Towuti with hydrodynamic and biogeochemical models. The results expand our knowledge of tropical lakes' mixing and stratification and the resultant chemical dynamics.

The hydrodynamic simulations suggest that, for thermogenically stratified tropical lakes, their stratification status is determined by local climate conditions and lake morphology. Among the climate variables, air temperature has the most significance. Air temperature strongly controls the surface heat flux, determining whether the surface of the lake cools down sufficiently to initiate thermal convection. Wind speed is the second most important factor. It affects both the heat flux and the momentum flux in a lake. A change in surface heat flux that eliminates the established thermal gradient (i.e. when lake surface cools down to bottom water temperature) causes the whole water column to mix through thermal convection, but the process proceeds slower than overturns in temperate lakes. The bathymetry of a tropical lake also influences its mixing status. For lakes in the same climate, such as neighboring Lakes Towuti and Matano, mixing status is mainly determined by their depths. For stable stratification, the depth of a lake needs to significantly exceed the typical thermocline depth. Large thermogenically stratified

tropical lakes tend to have stable thermoclines at depths around 80 m (Katsev et al., 2017). Thus, stratification in lakes shallower than 100 m is susceptible to annual variations in weather, and may be mixed frequently. Lakes between 100 m to 200 m deep are likely to be oligomictic. Lakes deeper than 200 m are likely to be meromictic. Changes in lake depth in response to changes in climate thus can lead to changes in stratification regime. In particular, for Lake Towuti, the cooler, drier, and windier conditions during the LGM, which likely decreased the water level to around 150 m, must have induced frequent mixing and oxygenation of the bottom waters. This agrees well with paleolimnological evidence (Vogel et al., 2015, Goudge et al., 2017).

Lakes' mixing regimes regulate their chemical properties. In lakes that sustain stratification for many years, oxygen becomes consumed in the deeper layers, even under oligotrophic conditions. For Lake Towuti, the transition from full oxygenation (with oxygen in deeper waters approaching saturation levels) to deep-water anoxia is suggested by the simulations to take about 30 years. The anoxia allows the accumulation of reduced species, such as hydrogen sulfide, ferrous iron, and methane. Abundances of sulfur vs. iron minerals in the lake's bedrock and catchment determine whether sulfide or ferrous iron would dominate. For Malili Lake system, the catchment bedrock is dominated by ultramafic species who provide abundant iron sources into the lake, suggesting the tendency of Lake Matano and Lake Towuti being ferruginous lakes.It remains an interesting question whether the balance between the iron-rich conditions (ferruginous) and the sulfide-rich conditions (euxinic) is unstable, i.e. whether accumulation of either substance tends to further promote its accumulation at the expense of another. The abundance of iron suppresses the production of sulfide, by precipitating it out with Fe^{2+} as FeS, by oxidizing it with reactive FeIII and precipitating it out as elemental sulfur (S_0), or by encouraging the abundance of iron reducers that compete with sulfate reducers for the organic metabolic substrates. Our simulations suggest that coexistence of Fe^{2+} and H_2S is

possible at low ($\mu mol\,L^{-1}$) concentrations, as observed in Lake Towuti. This balance between Fe^{2+} and H_2S is made possible by episodic weak ventilation of the deep waters, which limits the concentration of ferrous iron and resets the reduced species concentrations to low levels.

The simulation results of the chemistry model suggest that it takes at least one-month of persisted mixing to reintroduce oxygen into the bottom layer of Lake Towuti, or similar stratified tropical lakes. This rate is slower than what is typically observed in mid-latitude lakes, where the convection process transports oxygen at a much quicker rate. Thus, it is possible that lake Towuti might experience a periodical mixing event that homogenizes water temperature without completely ventilating the water bottom. Although anoxia conditions are observed from 2013 to 2015, it is possible for Lake Towuti to experience full water column mixing immediately before this.

The length of stratification and anoxia have important implications on the primary productivity of a lake. On one side, stratification can limit the availability of nutrients at the lake surface and limit plankton's primary production. On the other hand, the stratification can lead to oxygen depletion and results in reduced environment at the lake bottom, releasing the phosphorus trapped by iron oxides at the lake sediments, introducing nutrients to the water column to enhance the water column primary production. The net effect is related to the initial phosphorus concentration in the water column and sediment. Thus the variations in climate conditions and changes in lake stability have profound influence on its primary production.

Chapter 5

Bibliography

Ageli, M. K., Hamilton, P. B., Bramburger, A. J., Weidman, R. P., Song, Z., Russell, J., Vogel, H., Bijaksana, S., and Haffner, G. D. Benthic-Pelagic state changes in the primary trophic level of an ancient tropical lake. *Palaeogeography, Palaeoclimatology, Palaeoecology*, 594 (March):110937, 2022. ISSN 00310182. doi: 10.1016/j.palaeo.2022.110937.

Ajayi, T. and Gupta, I. A review of reactive transport modeling in wellbore integrity problems. *Journal of Petroleum Science and Engineering*, 175(January):785–803, 2019. ISSN 09204105. doi: 10.1016/j.petrol.2018.12.079.

Albritton, D. L., Filho, L. G. M., Cubasch, U., Dai, X., Ding, Y., Griggs, D. J., Hewitson, B., Isaksen, I., Karl, T., McFarland, M., Meleshko, V. P., Mitchell, J. F. B., Noguer, M., Nyenzi, B. S., Oppenheimer, M., Penner, J. E., Pollonais, S., Stocker, T., Trenberth, K. E., Allen, M. R., Baede, A. P. M., Church, J. A., Ehhalt, D. H., Folland, C. K., Giorgi, F., Gregory, J. M., Haywood, J. M., House, J. I., Hulme, M., Jaramillo, V. J., Jayaraman, A., Johnson, C. A., Joussaume, S., Karoly, D. J., Kheshgi, H., Quéré, C. L., Mata, L. J., McAvaney, B. J., Mearns, L. O., Meehl, G. A., Iii, B. M., Mugara, R. K., Prather, M., Prentice, C., Ramaswamy, V., Raper, S. C. B., Salinger, M. J., Wang, M.-X., Watson, R. T., Yap, K.-S., Joos, F., Ramirez-Rojas, A., Stone, J. M. R., and Zillman, J. 2001: Observed Climate Variability and Change. In *Climate Change 2001: The Scientific Basis. Contribution of Working Group I to the Third Assessment Report of the Intergovernmental Panel on Climate Change*. Cambridge University Press, Cambridge, United Kingdom, 2001.

Alcocer, J. Mexican Meromictic Lakes: What We Know So Far. In Gulati, R. D., Zadereev, E. S., and Degermendzhi, A. G., editors, *Ecology of Meromictic Lakes*, volume 228, pages 353–375. Springer International Publishing, Cham, 2017. ISBN 978-3-319-49141-7 978-3-319-49143-1. doi: 10.1007/978-3-319-49143-1_12.

Alin, S. R. and Johnson, T. C. Carbon cycling in large lakes of the world: A synthesis of

production, burial, and lake-atmosphere exchange estimates. *Global Biogeochemical Cycles*, 21(3):1–12, 2007. ISSN 08866236. doi: 10.1029/2006GB002881.

Anderson, R. Y. *Meromictic Lakes and Varved Lake Sediments in North America*. U.S. Government Printing Office, 1985.

As-syakur, A. R., Adnyana, I. W. S., Mahendra, M. S., Arthana, I. W., Merit, I. N., Kasa, I. W., Ekayanti, N. W., Nuarsa, I. W., and Sunarta, I. N. Observation of spatial patterns on the rainfall response to ENSO and IOD over Indonesia using TRMM Multisatellite Precipitation Analysis (TMPA). *International Journal of Climatology*, 34(15):3825–3839, 2014. ISSN 1097-0088. doi: 10.1002/joc.3939.

Austin, J. and Colman, S. A century of temperature variability in Lake Superior. *Limnology and Oceanography*, 53(6):2724–2730, 2008. ISSN 1939-5590. doi: 10.4319/lo.2008.53.6.2724.

Bärenbold, F., Kipfer, R., and Schmid, M. Dynamic modelling provides new insights into development and maintenance of Lake Kivu's density stratification. *Environmental Modelling & Software*, 147:105251, January 2022. ISSN 1364-8152. doi: 10.1016/j.envsoft.2021.105251.

Berner, R. A. A New Geochemical Classification of Sedimentary Environments. *SEPM Journal of Sedimentary Research*, Vol. 51, 1981. ISSN 1527-1404. doi: 10.1306/212F7C7F-2B24-11D7-8648000102C1865D.

Boehrer, B., von Rohden, C., and Schultze, M. Physical Features of Meromictic Lakes: Stratification and Circulation. In *Ecology of Meromictic Lakes*, pages 15–34. Springer, Cham, 2017. doi: 10.1007/978-3-319-49143-1_2.

Canfield, D. E. and Thamdrup, B. Towards a consistent classification scheme for geochemical environments, or, why we wish the term 'suboxic' would go away: Editorial. *Geobiology*, 7 (4):385–392, 2009. ISSN 14724677. doi: 10.1111/j.1472-4669.2009.00214.x.

Chen, C.-T. A. and Millero, F. J. Thermodynamic Properties for Natural Waters Covering Only the Limnological Range. *Limnology and Oceanography*, 31(3):657–662, 1986. ISSN 19395590. doi: 10.4319/lo.1986.31.3.0657.

Chitamwebwa, D. B. R. Meromixis, stratification and internal waves in Kigoma waters of Lake Tanganyika. In Lindqvist, O. V., Mölsä, H., Salonen, K., and Sarvala, J., editors, *From Limnology to Fisheries: Lake Tanganyika and Other Large Lakes*, pages 59–64. Springer Netherlands, Dordrecht, 1999. ISBN 978-90-481-5339-8 978-94-017-1622-2. doi: 10.1007/978-94-017-1622-2_5.

Costa, K. M., Russell, J. M., Vogel, H., and Bijaksana, S. Hydrological connectivity and mixing of Lake Towuti, Indonesia in response to paleoclimatic changes over the last 60,000 years. *Palaeogeography, Palaeoclimatology, Palaeoecology*, 417:467–475, 2015. ISSN 00310182. doi: 10.1016/j.palaeo.2014.10.009.

Crowe, S. A., Katsev, S., Leslie, K., Sturm, A., Magen, C., Nomosatryo, S., Pack, M. A., Kessler, J. D., Reeburgh, W. S., Roberts, J. A., González, L., Douglas Haffner, G., Mucci, A., Sundby, B., and Fowle, D. A. The methane cycle in ferruginous Lake Matano. *Geobiology*, 9(1):61–78, January 2011. ISSN 14724677. doi: 10.1111/j.1472-4669.2010.00257.x.

Damanik, A., Wille, M., Ahmad, Q., Russell, J. M., Bijaksana, S., Cahyarini, S. Y., and Vogel, H. Mo isotope variability records climate-driven water column redox changes in ferruginous Lake Towuti , Indonesia over the past ˜ 30 kyrs. In *EGU General Assembly 2022*, Vienna, Austria, 2022.

De Crop, W. and Verschuren, D. Mixing regimes in the equatorial crater lakes of western Uganda. *Limnologica*, 90:125891, September 2021. ISSN 0075-9511. doi: 10.1016/j.limno.2021.125891.

Engesgaard, P. and Christensen, T. H. A review of chemical solute transport models. *Nordic Hydrology*, 19(3):183–216, 1988. ISSN 00291277. doi: 10.2166/nh.1988.0013.

Fang, X. and Stefan, H. G. Long-term lake water temperature and ice cover simulations/measurements. *Cold Regions Science and Technology*, 24(3):289–304, July 1996. ISSN 0165-232X. doi: 10.1016/0165-232X(95)00019-8.

Firmansyah, A. J., Nurjani, E., and Sekaranom, A. B. Effects of the El Niño-Southern Oscillation (ENSO) on rainfall anomalies in Central Java, Indonesia. *Arabian Journal of Geosciences*, 15(24):1746, December 2022. ISSN 1866-7538. doi: 10.1007/s12517-022-11016-2.

Frey, D. G. A limnological reconnaissance of Lake Lanao. *SIL Proceedings, 1922-2010*, 17(2): 1090–1102, November 1969. ISSN 0368-0770. doi: 10.1080/03680770.1968.11895955.

Froelich, P. N., Klinkhammer, G. P., Bender, M. L., Luedtke, N. A., Heath, G. R., Cullen, D., Dauphin, P., Hammond, D., Hartman, B., and Maynard, V. Early oxidation of organic matter in pelagic sediments of the eastern equatorial Atlantic: Suboxic diagenesis. *Geochimica et Cosmochimica Acta*, 43(7):1075–1090, July 1979. ISSN 0016-7037. doi: 10.1016/0016-7037(79)90095-4.

Fukushima, T., Matsushita, B., Subehi, L., Setiawan, F., and Wibowo, H. Will hypolimnetic waters become anoxic in all deep tropical lakes? *Scientific Reports*, 7(1):45320, May 2017. ISSN 2045-2322. doi: 10.1038/srep45320.

Fukushima, T., Setiawan, F., Subehi, L., Jiang, D., and Matsushita, B. Water temperature and some water quality in Lake Toba, a tropical volcanic lake. *Limnology*, August 2022. ISSN 1439-8621, 1439-863X. doi: 10.1007/s10201-022-00703-4.

Gaudard, A., Råman Vinnå, L., Bärenbold, F., Schmid, M., and Bouffard, D. Toward an open access to high-frequency lake modeling and statistics data for scientists and practitioners – the

case of Swiss lakes using Simstrat v2.1. *Geosci. Model Dev.*, 12(9):3955–3974, September 2019. ISSN 1991-9603. doi: 10.5194/gmd-12-3955-2019.

Goudge, T. A., Russell, J. M., Mustard, J. F., Head, J. W., and Bijaksana, S. A 40,000 yr record of clay mineralogy at Lake Towuti, Indonesia: Paleoclimate reconstruction from reflectance spectroscopy and perspectives on paleolakes on Mars. *Bulletin of the Geological Society of America*, 129(7-8):806–819, 2017. ISSN 19432674. doi: 10.1130/B31569.1.

Goudsmit, G. H., Burchard, H., Peeters, F., and Wüest, A. Application of k-ε turbulence models to enclosed basins: The role of internal seiches. *Journal of Geophysical Research C: Oceans*, 107(12):23–1, 2002. ISSN 01480227. doi: 10.1029/2001jc000954.

Guilbaud, R., Poulton, S. W., Butterfield, N. J., Zhu, M., and Shields-Zhou, G. A. A global transition to ferruginous conditions in the early Neoproterozoic oceans. *Nature Geoscience*, 8(6):466–470, June 2015. ISSN 1752-0908. doi: 10.1038/ngeo2434.

Hambright, K. D., Gophen, M., and Serruya, S. Influence of long-term climatic changes on the stratification of a subtropical, warm monomictic lake. *Limnology and Oceanography*, 39(5): 1233–1242, 1994. ISSN 19395590. doi: 10.4319/lo.1994.39.5.1233.

Hasberg, A. K. M., Bijaksana, S., Held, P., Just, J., Melles, M., Morlock, M. A., Opitz, S., Russell, J. M., Vogel, H., and Wennrich, V. Modern sedimentation processes in Lake Towuti, Indonesia, revealed by the composition of surface sediments. *Sedimentology*, 66(2):675–698, February 2019. ISSN 00370746. doi: 10.1111/sed.12503.

Heiskanen, J. J., Mammarella, I., Ojala, A., Stepanenko, V., Erkkilä, K.-M., Miettinen, H., Sandström, H., Eugster, W., Leppäranta, M., Järvinen, H., Vesala, T., and Nordbo, A. Effects of water clarity on lake stratification and lake-atmosphere heat exchange. *Journal of Geophysical Research: Atmospheres*, 120(15):7412–7428, 2015. ISSN 2169-8996. doi: 10.1002/2014JD022938.

Hersbach, H., Bell, B., Berrisford, P., Hirahara, S., Horányi, A., Muñoz-Sabater, J., Nicolas, J., Peubey, C., Radu, R., Schepers, D., Simmons, A., Soci, C., Abdalla, S., Abellan, X., Balsamo, G., Bechtold, P., Biavati, G., Bidlot, J., Bonavita, M., De Chiara, G., Dahlgren, P., Dee, D., Diamantakis, M., Dragani, R., Flemming, J., Forbes, R., Fuentes, M., Geer, A., Haimberger, L., Healy, S., Hogan, R. J., Hólm, E., Janisková, M., Keeley, S., Laloyaux, P., Lopez, P., Lupu, C., Radnoti, G., de Rosnay, P., Rozum, I., Vamborg, F., Villaume, S., and Thépaut, J.-N. The ERA5 global reanalysis. *Quarterly Journal of the Royal Meteorological Society*, 146(730):1999–2049, 2020. ISSN 1477-870X. doi: 10.1002/qj.3803.

Hostetler, S. W. *Simulation of Lake Evaporation with an Energy Balance-Eddy Diffusion Model of Lake Temperature: Model Development and Validation, and Application to Lake-Level Variations at Harney-Malheur Lake, Oregon*. PhD thesis, University of Oregon, 1987.

Hutchinson, G. E. and Löffler, H. The Thermal Classification of Lakes. *Proceedings of the*

National Academy of Sciences, 42(2):84–86, 1956. ISSN 0027-8424. doi: 10.1073/pnas.42.2.84.

Idso, S. B. On the concept of lake stability. *Limnology and Oceanography*, 18(4):681–683, July 1973. ISSN 0024-3590. doi: 10.4319/lo.1973.18.4.0681.

Imboden, D. M. and Wüest, A. Mixing Mechanisms in Lakes. In Lerman, A., Imboden, D. M., and Gat, J. R., editors, *Physics and Chemistry of Lakes*, pages 83–138. Springer Berlin Heidelberg, Berlin, Heidelberg, 1995. ISBN 978-3-642-85132-2. doi: 10.1007/978-3-642-85132-2_4.

Jassby, A. and Powell, T. Vertical patterns of eddy diffusion during stratification in Castle Lake, California1. *Limnology and Oceanography*, 20(4):530–543, 1975. ISSN 1939-5590. doi: 10.4319/lo.1975.20.4.0530.

Joehnk, K. and Umlauf, L. Modelling the metalimnetic oxygen minimum in a medium sized alpine lake. *Ecological Modelling*, 136(1):67–80, January 2001. ISSN 03043800. doi: 10.1016/S0304-3800(00)00381-1.

Katsev, S. and Crowe, S. A. Organic carbon burial efficiencies in sediments: The power law of mineralization revisited. *Geology*, 43(7):607–610, 2015. ISSN 19432682. doi: 10.1130/G36626.1.

Katsev, S., Crowe, S. A., Mucci, A., Sundby, B., Nomosatryo, S., Douglas Haffner, G., and Fowle, D. A. Mixing and its effects on biogeochemistry in the persistently stratified, deep, tropical Lake Matano, Indonesia. *Limnology and Oceanography*, 55(2):763–776, March 2010. ISSN 00243590. doi: 10.4319/lo.2010.55.2.0763.

Katsev, S., Aaberg, A. A., Crowe, S. A., and Hecky, R. E. Recent Warming of Lake Kivu. *PLoS ONE*, 9(10):e109084, October 2014. ISSN 1932-6203. doi: 10.1371/journal.pone.0109084.

Katsev, S., Verburg, P., Llirós, M., Minor, E. C., Kruger, B. R., and Li, J. Tropical Meromictic Lakes: Specifics of Meromixis and Case Studies of Lakes Tanganyika, Malawi, and Matano. In *Ecology of Meromictic Lakes*, pages 277–323. Springer, Cham, 2017. doi: 10.1007/978-3-319-49143-1_10.

Kling, G. W., Tuttle, M. L., and Evans, W. C. The evolution of thermal structure and water chemistry in Lake Nyos. *Journal of Volcanology and Geothermal Research*, 39(2):151–165, November 1989. ISSN 0377-0273. doi: 10.1016/0377-0273(89)90055-3.

Kraemer, B. M., Anneville, O., Chandra, S., Dix, M., Kuusisto, E., Livingstone, D. M., Rimmer, A., Schladow, S. G., Silow, E., Sitoki, L. M., Tamatamah, R., Vadeboncoeur, Y., and McIntyre, P. B. Morphometry and average temperature affect lake stratification responses to climate change. *Geophysical Research Letters*, 42(12):4981–4988, 2015. ISSN 1944-8007. doi: 10.1002/2015GL064097.

Kranenburg, W., Tiessen, M., Veenstra, J., de Graaff, R., Uittenbogaard, R., Bouffard, D.,

Sakindi, G., Umutoni, A., Van de Walle, J., Thiery, W., and van Lipzig, N. 3D-modelling of Lake Kivu: Horizontal and vertical flow and temperature structure under spatially variable atmospheric forcing. *Journal of Great Lakes Research*, 46(4):947–960, 2020. ISSN 03801330. doi: 10.1016/j.jglr.2020.05.012.

Likongwe, P., Kihoro, J., Ngigi, M., and Jamu, D. Modeling spatial non-stationarity of Chambo in South-East Arm of Lake Malawi. *Asian Journal of Applied Science and Engineering*, 4 (2):81–90, 2015.

MacIntyre, S. and Melack, J. M. Meromixis in an equatorial African soda lake1. *Limnology and Oceanography*, 27(4):595–609, 1982. ISSN 1939-5590. doi: 10.4319/lo.1982.27.4.0595.

Mironov, D. V. Parameterization of lakes in numerical weather prediction: Description of a lake model. Technical Report 11, German Weather Service, O enbacham Main, Germany, August 2008.

Oleksy, I. A. and Richardson, D. C. Climate Change and Teleconnections Amplify Lake Stratification With Differential Local Controls of Surface Water Warming and Deep Water Cooling. *Geophysical Research Letters*, 48(5):e2020GL090959, 2021. ISSN 1944-8007. doi: 10.1029/2020GL090959.

Perroud, M., Goyette, S., Martynov, A., Beniston, M., and Anneville, O. Simulation of multiannual thermal profiles in deep Lake Geneva: A comparison of one-dimensional lake models. *Limnology and Oceanography*, 54(5):1574–1594, 2009. ISSN 00243590. doi: 10.4319/lo.2009.54.5.1574.

Poulton, S. W. and Canfield, D. E. Ferruginous conditions: A dominant feature of the ocean through Earth's history. *Elements*, 7(2):107–112, 2011. ISSN 18115217. doi: 10.2113/gselements.7.2.107.

Poulton, S. W., Fralick, P. W., and Canfield, D. E. The transition to a sulphidic ocean $\sim$ 1.84 billion years ago. *Nature*, 431(7005):173–177, September 2004. ISSN 1476-4687. doi: 10.1038/nature02912.

Rejmánková, E., Komárek, J., Dix, M., Komárková, J., and Girón, N. Cyanobacterial blooms in Lake Atitlan, Guatemala. *Limnologica*, 41(4):296–302, December 2011. ISSN 0075-9511. doi: 10.1016/j.limno.2010.12.003.

Richardson, D. C., Melles, S. J., Pilla, R. M., Hetherington, A. L., Knoll, L. B., Williamson, C. E., Kraemer, B. M., Jackson, J. R., Long, E. C., Moore, K., Rudstam, L. G., Rusak, J. A., Saros, J. E., Sharma, S., Strock, K. E., Weathers, K. C., and Wigdahl-Perry, C. R. Transparency, Geomorphology and Mixing Regime Explain Variability in Trends in Lake Temperature and Stratification across Northeastern North America (1975–2014). *Water*, 9 (6):442, June 2017. ISSN 2073-4441. doi: 10.3390/w9060442.

Rickard, D. The solubility of FeS. *Geochimica et Cosmochimica Acta*, 70(23):5779–5789, December 2006. ISSN 00167037. doi: 10.1016/j.gca.2006.02.029.

Russell, J. M., Bijaksana, S., Vogel, H., Melles, M., Kallmeyer, J., Ariztegui, D., Crowe, S., Fajar, S., Hafidz, A., Haffner, D., Hasberg, A., Ivory, S., Kelly, C., King, J., Kirana, K., Morlock, M., Noren, A., O'Grady, R., Ordonez, L., Stevenson, J., von Rintelen, T., Vuillemin, A., Watkinson, I., Wattrus, N., Wicaksono, S., Wonik, T., Bauer, K., Deino, A., Friese, A., Henny, C., Imran, Marwoto, R., Ngkoimani, L. O., Nomosatryo, S., Safiuddin, L. O., Simister, R., and Tamuntuan, G. The Towuti Drilling Project: Paleoenvironments, biological evolution, and geomicrobiology of a tropical Pacific lake. *Scientific Drilling*, 21 (July):29–40, 2016. ISSN 18163459. doi: 10.5194/sd-21-29-2016.

Russell, J. M., Vogel, H., Bijaksana, S., Melles, M., Deino, A., Hafidz, A., Haffner, D., Hasberg, A. K., Morlock, M., von Rintelen, T., Sheppard, R., Stelbrink, B., and Stevenson, J. The late quaternary tectonic, biogeochemical, and environmental evolution of ferruginous Lake Towuti, Indonesia. *Palaeogeography, Palaeoclimatology, Palaeoecology*, 556(August), 2020. ISSN 00310182. doi: 10.1016/j.palaeo.2020.109905.

Sahoo, G. B., Forrest, A. L., Schladow, S. G., Reuter, J. E., Coats, R., and Dettinger, M. Climate change impacts on lake thermal dynamics and ecosystem vulnerabilities. *Limnology and Oceanography*, 61(2):496–507, 2016. ISSN 19395590. doi: 10.1002/lno.10228.

Shakeri Yekta, S., Svensson, B. H., Björn, A., and Skyllberg, U. Thermodynamic modeling of iron and trace metal solubility and speciation under sulfidic and ferruginous conditions in full scale continuous stirred tank biogas reactors. *Applied Geochemistry*, 47:61–73, 2014. ISSN 18729134. doi: 10.1016/j.apgeochem.2014.05.001.

Sigurdsson, H., Devine, J. D., Tchua, F. M., Presser, F. M., Pringle, M. K. W., and Evans, W. C. Origin of the lethal gas burst from Lake Monoun, Cameroun. *Journal of Volcanology and Geothermal Research*, 31(1):1–16, March 1987. ISSN 0377-0273. doi: 10.1016/0377-0273(87)90002-3.

Skeel, R. D. and Berzins, M. A Method for the Spatial Discretization of Parabolic Equations in One Space Variable. *SIAM Journal on Scientific and Statistical Computing*, 11(1):1–32, January 1990. ISSN 0196-5204, 2168-3417. doi: 10.1137/0911001.

Sommer, T., Schmid, M., and Wüest, A. The role of double diffusion for the heat and salt balance in Lake Kivu. *Limnology and Oceanography*, 64(2):650–660, 2019. ISSN 19395590. doi: 10.1002/lno.11066.

Stepanenko, V. and Lykossov, V. Numerical modeling of the heat and moisture transport in a lake-soil system. *Russian Journal for Meteorology and Hydrology*, (3):95–104, January 2005.

Stepanenko, V. M., Goyette, S., Martynov, A., Perroud, M., Fang, X., and Mironov, D. First

steps of a Lake Model intercomparison project: LakeMIP. *Boreal Environment Research*, 15 (2):191–202, 2010. ISSN 12396095.

Stetler, J. T., Girdner, S., Mack, J., Winslow, L. A., Leach, T. H., and Rose, K. C. Atmospheric stilling and warming air temperatures drive long-term changes in lake stratification in a large oligotrophic lake. *Limnology and Oceanography*, 66(3):954–964, 2021. ISSN 19395590. doi: 10.1002/lno.11654.

Subin, Z. M., Riley, W. J., and Mironov, D. An improved lake model for climate simulations: Model structure, evaluation, and sensitivity analyses in CESM1. *Journal of Advances in Modeling Earth Systems*, 4:M02001, February 2012. ISSN 1942-2466. doi: 10.1029/2011MS000072.

Sulistioadi, Y. B., Tseng, K.-H., Shum, C. K., Hidayat, H., Sumaryono, M., Suhardiman, A., Setiawan, F., and Sunarso, S. Satellite radar altimetry for monitoring small rivers and lakes in Indonesia. *Hydrology and Earth System Sciences*, 19(1):341–359, January 2015. ISSN 1027-5606. doi: 10.5194/hess-19-341-2015.

Supari, Tangang, F., Salimun, E., Aldrian, E., Sopaheluwakan, A., and Juneng, L. ENSO modulation of seasonal rainfall and extremes in Indonesia. *Climate Dynamics*, 51(7):2559–2580, October 2018. ISSN 1432-0894. doi: 10.1007/s00382-017-4028-8.

Swanner, E. D., Lambrecht, N., Wittkop, C., Harding, C., Katsev, S., Torgeson, J., and Poulton, S. W. The biogeochemistry of ferruginous lakes and past ferruginous oceans. *Earth-Science Reviews*, 211(June):103430, 2020. ISSN 00128252. doi: 10.1016/j.earscirev.2020.103430.

Taillefert, M. and Gaillard, J.-F. Reactive transport modeling of trace elements in the water column of a stratified lake: Iron cycling and metal scavenging. *Journal of Hydrology*, 256: 16–34, September 2001. doi: 10.1016/S0022-1694(01)00524-8.

Thiery, W., Stepanenko, V. M., Fang, X., Jöhnk, K. D., Li, Z., Martynov, A., Perroud, M., Subin, Z. M., Darchambeau, F., Mironov, D., and Van Lipzig, N. P. LakeMIP Kivu: Evaluating the representation of a large, deep tropical lake by a set of one-dimensional lake models. *Tellus, Series A: Dynamic Meteorology and Oceanography*, 66(1):1–18, 2014. ISSN 16000870. doi: 10.3402/tellusa.v66.21390.

Vaillant, J. J., Haffner, G. D., and Cristescu, M. E. The ancient lakes of indonesia: Towards integrated research on speciation. In *Integrative and Comparative Biology*, volume 51, pages 634–643. Oxford Academic, October 2011. doi: 10.1093/icb/icr101.

Verburg, P. and Hecky, R. E. The physics of the warming of Lake Tanganyika by climate change. *Limnology and Oceanography*, 54(6 PART 2):2418–2430, 2009. ISSN 00243590. doi: 10.4319/lo.2009.54.6_part_2.2418.

Vogel, H., Russell, J. M., Cahyarini, S. Y., Bijaksana, S., Wattrus, N., Rethemeyer, J., and Melles, M. Depositional modes and lake-level variability at Lake Towuti, Indonesia, during

the past ˜29 kyr BP. *Journal of Paleolimnology*, 54(4):359–377, September 2015. ISSN 15730417. doi: 10.1007/s10933-015-9857-z.

Vuillemin, A., Friese, A., Alawi, M., Henny, C., Nomosatryo, S., Wagner, D., Crowe, S. A., and Kallmeyer, J. Geomicrobiological features of ferruginous sediments from lake Towuti, Indonesia. *Frontiers in Microbiology*, 7(JUN):1007, 2016. ISSN 1664302X. doi: 10.3389/fmicb.2016.01007.

Walker, K. F. and Likens, G. E. Meromixis and a reconsidered typology of lake circulation patterns: With 3 tables in the text. *SIL Proceedings, 1922-2010*, 19(1):442–458, October 1975. ISSN 0368-0770. doi: 10.1080/03680770.1974.11896084.

Weinberger, S. and Vetter, M. Using the hydrodynamic model DYRESM based on results of a regional climate model to estimate water temperature changes at Lake Ammersee. *Ecological Modelling*, 244:38–48, 2012. ISSN 03043800. doi: 10.1016/j.ecolmodel.2012.06.016.

Woolway, R. I. and Merchant, C. J. Worldwide alteration of lake mixing regimes in response to climate change. *Nature Geoscience*, 12(4):271–276, April 2019. ISSN 17520908. doi: 10.1038/s41561-019-0322-x.

Woolway, R. I., Meinson, P., Nõges, P., Jones, I. D., and Laas, A. Atmospheric stilling leads to prolonged thermal stratification in a large shallow polymictic lake. *Climatic Change*, 141(4):759–773, April 2017. ISSN 1573-1480. doi: 10.1007/s10584-017-1909-0.

Woolway, R. I., Sharma, S., Weyhenmeyer, G. A., Debolskiy, A., Golub, M., Mercado-Bettín, D., Perroud, M., Stepanenko, V., Tan, Z., Grant, L., Ladwig, R., Mesman, J., Moore, T. N., Shatwell, T., Vanderkelen, I., Austin, J. A., DeGasperi, C. L., Dokulil, M., La Fuente, S., Mackay, E. B., Schladow, S. G., Watanabe, S., Marcé, R., Pierson, D. C., Thiery, W., and Jennings, E. Phenological shifts in lake stratification under climate change. *Nature Communications*, 12(1):1–11, 2021. doi: 10.1038/s41467-021-22657-4.

Wuest, A., Piepke, G., and Halfman, J. Combined effects of dissolved solids and temperature on the density stratification of Malawi. In *Paleoclimatology of the Eastern African Lakes*, pages 183–202. Gordon and Breach, Toronto, 1996.

Xie, S. P., Kosaka, Y., Du, Y., Hu, K., Chowdary, J. S., and Huang, G. Indo-western Pacific ocean capacitor and coherent climate anomalies in post-ENSO summer: A review. *Advances in Atmospheric Sciences*, 33(4):411–432, 2016. ISSN 02561530. doi: 10.1007/s00376-015-5192-6.

Appendix A

Glossary and Acronyms

Care has been taken in this thesis to minimize the use of jargon and acronyms, but this cannot always be achieved. This appendix contains a table of acronyms and their meaning.

A.1 Acronyms

Table A.1: Acronyms

Acronym	Meaning
CTD	Conductivity, Temperature, and Depth
TD	Temperature Difference
TDI	Temperature Difference Indicator
HC	Heat Content
HCI	Heat Content Indicator
SS	Schmidt Stability
SSI	Schmidt Stability Index

Continued on next page

Table A.1 – continued from previous page

Acronym	Meaning
WTD	Weakest Temperature Difference
MBF	Maximum Buoyancy Frequency (squared)
LGM	Last Glacial Maximum
ENSO	El Niño-Southern Oscillation
IPWP	Indo-Pacific Warm Pool
PDE	Partial Differential Equation
SR	Sulfate Reduction
IR	Iron Reduction

Appendix B

Hydrodynamic Modeling Parameters

Table B.1: Physical parameters

Parameter / Method	Unit	Value	Comment
Turbulence Model			$k-\varepsilon$
Stability Function			Quasi-equilibrium
Flux Condition			No flux
Use Filtered Wind			false
Seiche Normalization			integral
Wind Drag Model			Wüest and Lorke, 2003
Inflow Mode			Inflow is density-driven
Pressure Gradients			Bottom Friction
Ice Model			off
Snow Model			Off
Time Step	seconds	60	

Continued on next page

Table B.1 – continued from previous page

Parameter / Method	Unit	Value	Comment
Start Day		2001-09-25	
End Day		2016-12-31	
Latitude	°	-2	
Air Pressure	mbar	1010	
α_{seiche}	1	0.0011046	Fraction of wind energy which goes into seiche energy
Q_{N^2}	1	0.75	Fit parameter for distribution of seiche energy
c_d	1	0.002	Bottom drag coefficient
H_{geo}	$\mathrm{W\,m^{-2}}$	0	Geothermal heat flux
p_{sw_water}	1	0.8	Fit parameter for absorption of short wave radiation from sky
p_{lw}	1	0.95	Fit parameter for absorption of infrared radiation from sky
p_{windf}	1	1	Fit parameter for convective and latent heat fluxes
β_{sol}	1	0.3	Fraction of short-wave radiation directly absorbed as heat by water
Initial Seiche Energy	J	1×10^{10}	Initial seiche energy
c_μ	1	0.09	constant for calculating turbulent viscosity for momentum

Continued on next page

Table B.1 – continued from previous page

Parameter / Method	Unit	Value	Comment
c'_μ	1	0.072	constant for calculating turbulent diffusivity for temperature
σ_k	1	1	constant for calculating turbulent diffusivity for k
σ_ε	1	1.3	constant for calculating turbulent diffusivity for ε

Appendix C

Chemsitry Model

C.1 Model Description

The chemistry model is developed by Sergei Katsev and Itay Halevy (PNAS in prep). The following paragraphs explained the mechanism of this model.

The basis of this chemistry model is constructed by a system of partial differential equations represented in Eq. C.1. The solution is obtained with MATLAB pdepe solver (reference to Skeel and Berzins (1990)).

$$\frac{\partial C_j}{\partial t} = \frac{\partial}{\partial z}\left(K_z(z)\frac{\partial C_j}{\partial z}\right) - v_j\frac{\partial C_j}{\partial z} + \sum_i \nu_i R_{ij} \tag{C.1}$$

Here, $K_z(z)$ is the depth-dependent turbulent diffusivity, v_j is advection velocity, but in this case, only refers to the settling velocity. R_{ij} is the ith reaction rates for chemical species j. Its stoichiometric coefficient for chemical j is ν_i. Species considered for constructing the systems of equations includes POM, Ac, O_2, SO_4^{2-}, TS=H_2S + HS^-, FeOOH, Fe^{2+}, S^0, FeS, and the biomass of the microbial populations that catalyze the corresponding reactions: X_{IR}, X_{SR}, X_{CH4},

X_{S-AOM}, X_{Fe-AOM}. The reactions involved are listed in table C.2. DIC, ammonium, and pH are assumed to be constant. Microbial reactions are described in the following bioenergetic model.

The bioenergetic model describes the energy of microbial metabolism as:

$$\Delta G = \lambda_{cat} \Delta G_{cat} + \Delta G_{ana} \tag{C.2}$$

where ΔG_{cat} is the Gibbs free energy of catabolism process, which generates energy for microbial consumption, and ΔG_{ana} describes the anabolism process that microbes consume energy for building up biomass. ΔG is thus the energy being dissipated into the environment. λ_{cat} is the number of times a catabolism process is required to provide the energy needed for forming one C-mol of biomass with anabolism. Thus, the maximum growth yield by per mol of reaction is:

$$Y_{max} = \frac{1}{\lambda_{cat}} = \frac{\Delta G_{cat}}{\Delta G - \Delta G_{ana}} \tag{C.3}$$

Cell-specific cataboblic reaction rates (r) is a function of substrate (S) concentrations:

$$r = \frac{1}{X}\frac{dS}{dt} = F_K F_T \tag{C.4}$$

Where X is the biomass in C-mols. F_K is the kinetic factor, and F_T is the thermodynamic factor.

F_K depends on maximum cell-specific rate V_{max} and substrate concentrations:

$$F_K = V_{max} \prod \frac{S_i}{K_m^i + S_i} \tag{C.5}$$

F_T is formed based on Gibbs free energy of catabolic reaction and ATP energy release:

$$F_T = 1 - \exp\left(\frac{\Delta G_{cat} + m\Delta G_{ATP}}{\chi RT}\right) \tag{C.6}$$

Table C.1: Chemical model boundary conditions

Parameter	Value	Unit	Comment
top boundary			
$[O_2]$	200	$\mu mol l^{-1}$	fixed concentration of oxygen
$[SO_4]$	40	$\mu mol l^{-1}$	fixed concentration of sulfate
F^0_{FeIII}	950	$mmol/m^2/yr$	surface flux of FeIII
F^0_G	0.1	$mmol/m^2/yr$	surface flux of OM
bottom boundary			
F^{bottom}_{FeII}	frec*F^{bottom}_{FeIII}	$mmol/m^2/yr$	bottom flux of FeII
	*frec: fraction of FeIII being recycled, it is related to organic matter flux, Fe(III) flux, oxygen concentration, and H_2S concentration		

Thus, variations in chemical species (S) and biomass (X) can be expressed as :

$$\frac{dS_s}{dt} = A_{sm} r_{mb} X_b \tag{C.7}$$

$$\frac{dX_b}{dt} = \sum_n Y_{nm} r_{mb} X_b - \lambda(m_G) X_b \tag{C.8}$$

A_{sm} is the stoichiometric coefficient for substrate s in a catabolic reaction m. r_{mb} is the rate of this reaction. X_m is the active biomass involved in stimulating this reaction. Term $\sum_n Y_{nm} r_{mb} X_b$ describes the yield of biomass X_b associated with anabolic reaction n and catabolic reaction m. Term $-\lambda(m_G) X_b$ on the other hand, describes the death of microbes related to the maintenance energy m_G.

The important boundary conditions of the model are illustrated in Fig. C.1 and are defined in Table C.1. Chemicals not mentioned here have surface boundary conditions of zero concentration for dissolved species and zero flux for particulate species. The bottom boundary conditions are zero flux for dissolved species. Solid species sink out when they reach the sediment-water interface at their settling rate defined by v_{settle} in Table C.4. A fraction of Fe(III) precipitated into the sediment is reduced and recycled as Fe^{2+}.

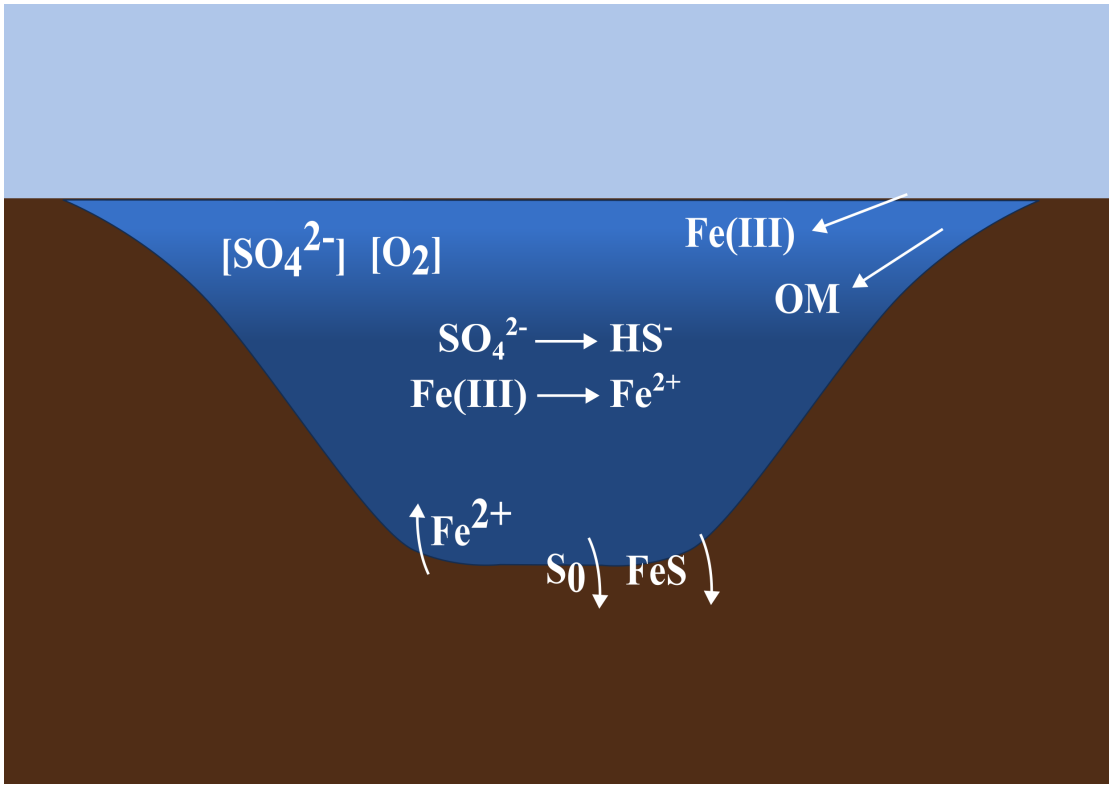

Figure C.1: Illustration of the important boundary conditions and reactions of the biogeochemistry model.

The primary production is assumed to be distributed in the upper water column according to an analytical exponential function:

$$PP(z) = PP_{total} k e^{-kz} \tag{C.9}$$

where $k = 0.0655$, assuming the abundance of primary production decreases at the same rate as light attenuation. PP_0 is 8300 μmol/L/yr, the total primary production of the lake integrated with depth. This is an assumption based on Lake Towuti being an oligotrophic lake. This process produces POM, which remineralizes following a power law of organic age and available

oxygen level (Katsev and Crowe, 2015):

$$k(z,[\mathrm{O}_2]) = fk_{ox} + (1-f)k_{anox} \tag{C.10}$$

where the partitioning coefficient is $f = [O2]/(K_{O2} + [O2])$. The reactivities for the oxic and anoxic mineralization are (Katsev and Crowe, 2015):

$$k_{ox} = 10^{-0.312}\tau^{-0.977} \tag{C.11}$$

$$k_{anox} = 10^{-1.1}\tau^{-0.857} \tag{C.12}$$

The age τ of organic material (in years) was calculated at each depth as:

$$\tau = \tau_{init} + \int_0^z \frac{dz}{v_{diff} + v_{settleG}} \tag{C.13}$$

Where v_{diff} is the effective downward velocity of organic matter, due to turbulent diffusion, which can be approximated as:

$$v_{diff} = \frac{1}{\frac{z}{K_z} - (\frac{z}{2K_z})^2 \ \frac{\partial K_z}{\partial z}} \tag{C.14}$$

$v_{settleG}$ is the linear settling velocity of organic matter, defined in Table C.4.

C.2 Biogeochemical Model Reactions

Table C.2: Chemical model reactions

Reaction	ΔG^0	Comment
$POM \longrightarrow CH_3COO^-$		hydrolysis
$CH_3COO^- + 2\,O_2 \longrightarrow 2\,HCO_3{}^- + H^+$		remineralisation
$SO_4{}^{2-} \xrightarrow{SulfateReducer} HS^-$		sulfate reduction
$FeOOH \xrightarrow{IronReducer} Fe^{2+}$		iron reduction
$SO_4^{2-} + CH_4 \longrightarrow HS^- + HCO_3^- + H_2O$	-33	anaerobic oxidation of methane (via sulfate)
$8\,FeOOH + CH_4 + 15\,H^+ \longrightarrow 8\,Fe^{2+} + HCO_3{}^- + 13\,H_2O$	-117	anaerobic oxidation of methane (via iron oxides)
$H_2S + 2\,O_2 \longrightarrow SO_4{}^{2-} + 2\,H^+$	-830	sulfide oxidation
$4\,Fe^{2+} + O_2 + 6\,H_2O \longrightarrow 4\,FeOOH + 8\,H^+$	-371	iron oxidation
$2\,FeOOH + H_2S + 4\,H^+ \longrightarrow S^0 + 2\,Fe^{2+} + 4\,H_2O$	-32	sulfide oxidation via iron oxides
$Fe^{2+} + HS^- \longrightarrow FeS + H^+$		precipitation
$4\,S^0 + 4\,H_2O \longrightarrow SO_4{}^{2-} + 3\,HS^- + 5\,H^+$	+55	

C.3 Biogeochemical Model Reaction Rates

Table C.3: Chemical reaction rates

Rate
$R_{PPO2} = R_{PP}$
$R_G = k(z, [\mathrm{O_2}])[POM]$
$R_{O2} = R_G \dfrac{[\mathrm{O_2}]}{[\mathrm{O_2}] + K_{O2}}$
$R_{HSox} = k_{HSox}[\mathrm{H_2S}][\mathrm{O_2}]$
$R_{Feox} = k_{Feox}[\mathrm{Fe^{2+}}][\mathrm{O_2}]$
$R_{HSFeIII} = k_{HSFeIII}[\mathrm{FeOOH}][\mathrm{H_2S}]$
$R_{FeS} = 5 \times 10^2 * (\Omega_{FeS} - 1)$ where $\Omega_{FeS} = \dfrac{[\mathrm{Fe^{2+}}][\mathrm{HS}]}{[\mathrm{H^+}]K_{FeS}}$ $\mathrm{HS} = \dfrac{[\mathrm{H_2S}]}{1 + [\mathrm{H^+}]/K_{HS}}$
$R_{CH4ox} = k_{CH4ox}[\mathrm{CH_4}][\mathrm{O_2}]$
$R_{disp} = k_{disp}[\mathrm{S^0}]$

C.4 Biogeochemical Model Parameters

Table C.4: Chemical model parameters

Parameter	Value	Unit	Comment
τ_{init}	0.5	y	initial age of organic matter
PP	22	mmol/m2/d	gross primary production
KAc	5	uM	affinity for acetate for SR
	15.5	uM	affinity for acetate for IR
	12	uM	affinity for acetate for methanogens
KO2	2	uM	affinity for oxygen
KO2inh	1	uM	inhibition of anaerobes by O_2
KSO4	5	uM	affinity for sulfate
KCH4	30	uM	affinity for methane (for AOM)
KFeIII	1000	uM	affinity for goethite
KFeR	20	uM	affinity for nanophase precipitates
KHS	9.3E-8	uM	acid dissociation constant for H_2S
KFeS	2.5E-3	uM	affinity for iron sulfide
v_{settle}	1800	m/y	settling velocity
$v_{settleG}$	600	m/y	settling velocity for organic matter
f_{rec}	0.1		constant related to fraction of FeIII being recycled from the sediment
kHSox	1	1/uM/y	rate constant
kFeox	1	1/uM/y	
kHSFeIII	2×10^{-1}	1/uM/y	
kFeS	5×10^{-1}	1/uM/y	
kCH4ox	1	1/uM/y	
kdisp	2×10^{-2}	1/y	
T	29	^{o}C	Temperature

Continued on next page

Table C.4 – continued from previous page

Parameter	Value	Unit	Comment
pH	7		pH
ΔG_{ATP}	30	kJ/mol	cost of producing ATP (for F_T)
χ	8,6,2	-	stoich. number of Jin&Bethke
m	1,5/4,1/4	-	stoich. number of Jin&Bethke
V_{max}	1.0	$mol_{rx}/mol_x/h$	microbial kinetics for SR
	$\times$ 1/10		microbial kinetics for IR
	$\times$ 1.0		microbial kinetics for meth.
	$\times$ 1/25		microbial kinetics for S-AOM
	$\times$ 3/10		microbial kinetics for Fe-AOM
	$\times$ 1/50		microbial kinetics for FeR-AOM
λ_{death}	2E-4	1/h	death constant
k_{death}	2E-3	1/h	death rate from energy starvation
P_{maint}	4.56	$kJ/mol_x/h$	min. maintenance power
Kanalim	1E-2	uM	limiting conc. for anabolism
HCO_3^-	3E-3	M	
NH_4^+	1E-5	M	nutrient for anabolism

Appendix D

Extra Figures

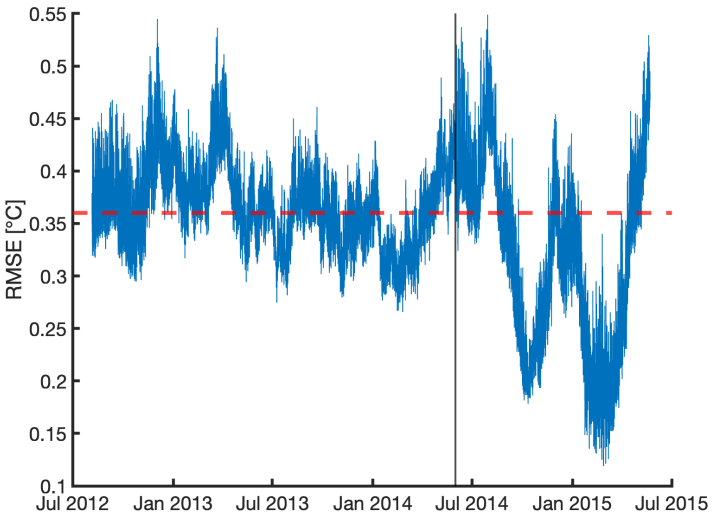

Figure D.1: Root mean squared error (RMSE) between model and mooring (2012 - 2015) temperature data as a function of time. The dashed line indicates an average RMSE of the dataset. The solid vertical line represents June 2014. After this time, the confidence in mooring data decreased. This figure illustrates that, RMSE significantly increased during 2012-2013 wet season. However, this increasing of error did not accumulate in the proceeding simulation.

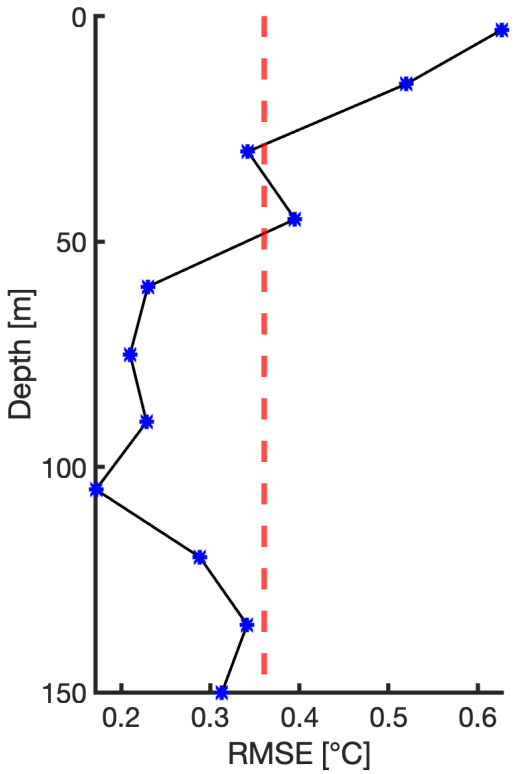

Figure D.2: RMSE between model and mooring (2012 - 2015) temperature data as a function of depth. Dashed line indicates the overall RMSE of the dataset. RMSE is larger than average at the surface, and is minimal at around 100 m. This indicates that Simstrat simulation errors are mostly observed at the surface rather than deeper part of the lake and that the modeling of surface heat flux over Lake Towuti results in discrepancy between simulation and observation. Bottom temperature simulated by simstrat is more satisfactory.

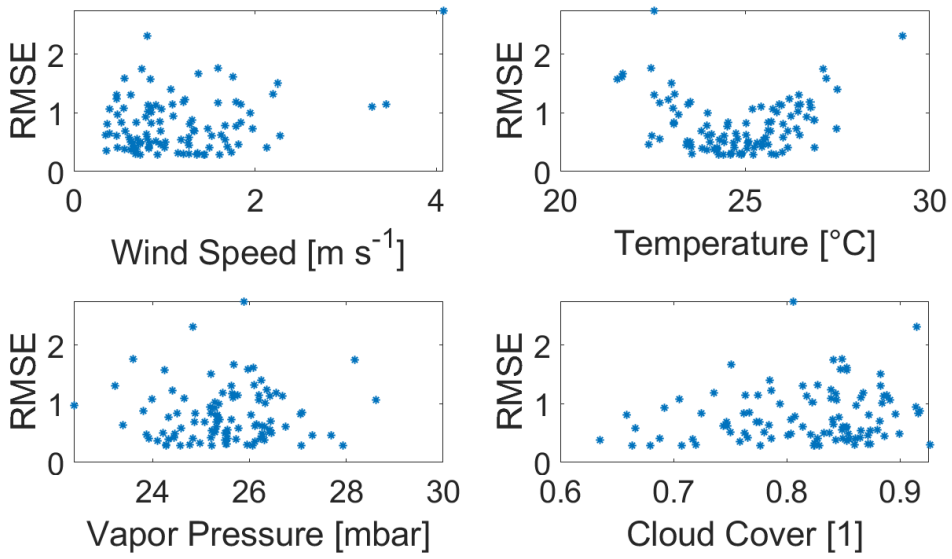

Figure D.3: RMSE sensitivity with meteorological variables. This figure is generated with the same data in 2.13, except the y-axis is now plotting the RMSE between the model and mooring data. This figure illustrates that the current configuration of meteorological variables is a satisfactory representation that allows simulation agreement with observation. No better combinations of meteorology can significantly improve the performance of the model.

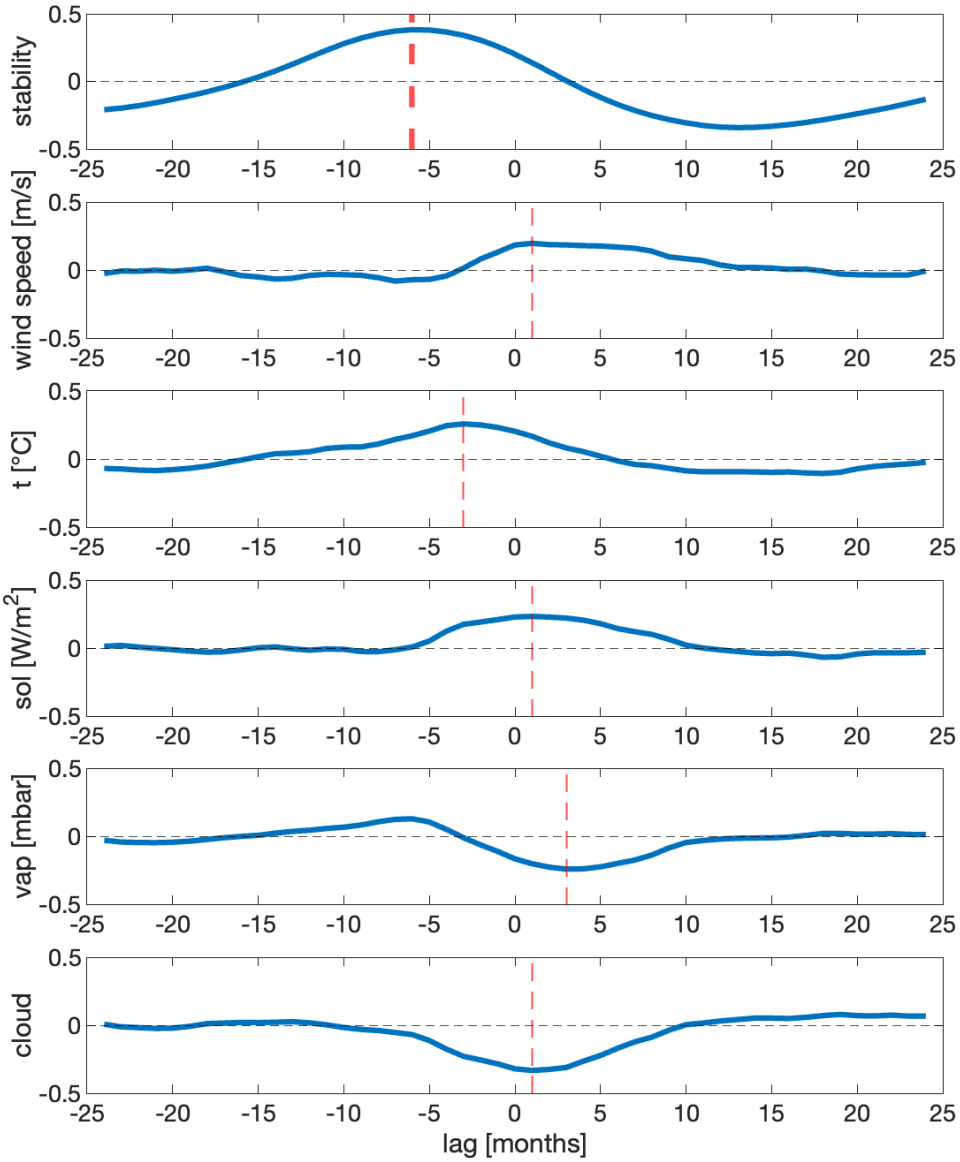

Figure D.4: Cross correlation between meteorological variables and MEI.v2 index. negative lag indicates MEI.v2 is prior to the local meteorological variable. The correlations are mostly weak (with Pearson's r smaller than 0.5 for all the climate variables). MEI.v2 index represents the air temperature over Lake Towuti several months later, but has delays in representing the wind speed, solar radiation, vapor pressure, and cloud cover over Lake Towuti.